NTNU

Norwegian University of
Science and Technology

Simulation of hydraulic transients of operation at two hydro power plants

Bjarne Vaage

MASTER THESIS

for

Student
Bjarne Vaage

Spring 2016

Simulation of hydraulic transients of operation at two hydro power plants

Simulering av hydrauliske transienter ved drift av to vannkraftverk

Background and objective

The prediction of hydraulic transient responses to hydro power operation can originate from many different objectives. One such objective is to establish the Fault-Ride-Through (FRT) behaviour of a power plant. Another objective is to evaluate the hydraulic response to an operation different to what the power plant has been designed for.
In the middle part of Norway there are two very different hydro power plant situated less that 14 km apart; Bruvollelva power plant (a small run-of-river hydro power plant) and Bogna power plant (a 56 MW single turbine unit with large reservoirs on either side). SINTEF Energy research have initiated investigations to identify the FRT properties of Bruvollelva power plant, whereas CEDREN has investigated the possible expansion with pumping capabilities and operation at Bogna. Principally, the simulations of hydraulic transients needed for both these cases can be performed using the same, generic simulation program.

The objective of the master thesis will be to simulate both these cases using the same simulation program; FRT properties of Bruvollelva Power plants as well as pumped storage operation at an expansion of Bogna in a future scenario of high wind energy penetration in the Norwegian electrical grid.

The following tasks are to be considered:

1. Literature review on hydraulic transient simulations on hydraulic power plants
2. Measure the hydraulic pressure at Bruvollelva Power plant during FRT test, if performed in time
3. Simulate FRT properties and compare this to measurements performed at Bruvollelva Power plant
4. Expand the simulation program so that it can perform simulations of operation at Bogna Power plant, both at the existing plant and for a possible future expansion.
5. Perform simulations of operation at Bogna power plant both at the existing plant and for a possible future expansion.

-- ” --

Within 14 days of receiving the written text on the master thesis, the candidate shall submit a research plan for his project to the department.

When the thesis is evaluated, emphasis is put on processing of the results, and that they are presented in tabular and/or graphic form in a clear manner, and that they are analyzed carefully.

The thesis should be formulated as a research report with summary both in English and Norwegian, conclusion, literature references, table of contents etc. During the preparation of the text, the candidate should make an effort to produce a well-structured and easily readable report. In order to ease the evaluation of the thesis, it is important that the cross-references are correct. In the making of the report, strong emphasis should be placed on both a thorough discussion of the results and an orderly presentation.

The candidate is requested to initiate and keep close contact with his/her academic supervisor(s) throughout the working period. The candidate must follow the rules and regulations of NTNU as well as passive directions given by the Department of Energy and Process Engineering.

Risk assessment of the candidate's work shall be carried out according to the department's procedures. The risk assessment must be documented and included as part of the final report. Events related to the candidate's work adversely affecting the health, safety or security, must be documented and included as part of the final report. If the documentation on risk assessment represents a large number of pages, the full version is to be submitted electronically to the supervisor and an excerpt is included in the report.

Pursuant to "Regulations concerning the supplementary provisions to the technology study program/Master of Science" at NTNU §20, the Department reserves the permission to utilize all the results and data for teaching and research purposes as well as in future publications.
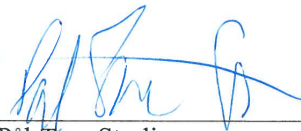
The final report is to be submitted digitally in DAIM. An executive summary of the thesis including title, student's name, supervisor's name, year, department name, and NTNU's logo and name, shall be submitted to the department as a separate pdf file. Based on an agreement with the supervisor, the final report and other material and documents may be given to the supervisor in digital format.

☐ Work to be done in lab (Water power lab, Fluids engineering lab, Thermal engineering lab)
☒ Field work

Department of Energy and Process Engineering, 13. January 2016

Olav Bolland
Department Head

Pål-Tore Storli
Academic Supervisor

Research Advisor:
Torbjørn Nielsen

Preface

This thesis came to life at the Waterpower Laboratory at NTNU during the spring of 2016. The thesis had two main objectives: to model and simulate hydraulic transients at Bogna power plant and to preform Fault Ride Through simulations at Bruvollelva power plant. In addition to this some physical measurements were preformed at Bruvollelva.

I sincerely hope that my work may be of use to future students. I set out planning to make simulations of hydro power plants more accessible for those of you who come after me. I am not sure I succeeded but if you find yourself stuck somewhere in my implementations, please contact me and I will try to guide you to the best of my knowledge.

My supervisor Pål-Tore Storli deserves a big thank you for always being there, answering my more or less (for the most part less) intelligent questions. This also goes for Professor Torbjørn Nielsen for providing me with invaluable information about his own turbine model. I would also like to thank the guys in the lab for aiding me when I had no clue what instruments to use in the field. And to my fellow students here at the Waterpower Laboratory who has made this year one to remember.

Last but not least Vigdis deserves a huge thank you for always supporting me the last five months. You made all of this much more cheerful.

Bjarne Vaage

Trondheim, June 9, 2016

Samandrag

Kraftproduksjonen i Europa går mot eit grønt skifte. Energiproduksjonen frå fornybare energikjelder som sol- og vindkraft aukar for kvar dag som går. Dette fører dog med seg eit par problem. Energi produsert av vind og sol bidrar ikkje til å oppretthalde og stabilisere nettfrekvensen i same grad som energi frå kol og gass. Dette kan føre til ein kvardag med større variasjonar i nettfrekvens enn det ein er vane med i dag. Desse variasjonane vil forplante seg via generator og inn til turbin og vassveg i kraftverka. Oppgåva tar for seg Bogna kraftverk i Snåsa for å sjekke om slike variasjonar i frekvensen vil påverke kraftverket i stor grad.

Som ein del av det grøne skiftet har ein i Noreg bygd ut store mengder småkraft. Med innførslene av nye nettkoder som skal passe betre saman med resten av Europa blir det stilt spørsmål om kor godt desse er rusta for å tåle små avvik i nettspenning. Oppgåva tar for seg Bruvollelva Småkraftverk som i samarbeid med SINTEF er testa for nettopp desse små spenningsavvika.

Det er gjennomført transiente simuleringar på begge kraftverka. Karakteristikk-metoden som er beskrive av *Wilye & Streeter* er implementert i det grafiske programmeringsspråket *Simulink*, som er basert på MATLAB. Dei fleste typiske element i eit vasskraftverk er implementert, frå inntak til utløp via vassvegar, svingearrangement, bekkeinntak, generator og turbin. Turbin og generator er regulert ved hjelp av klassiske PI-regulartorer. I tillegg til simuleringar er det også gjennomført måling på turbintrykket ved Bruvollelva.

Målingane ved den siste felt-testen ved Bruvollelva viste eit ganske overraskande resultat med eit trykkforløp som kan minne om eit fullt trykkstøt. Dette resultatet var forsøkt simulert utan hell. Dei simulerte resultata gjer eit mindre dramatisk forløp.

Simulering av Bogna fekk fram at kraftverket ikkje blir påverka i stor grad av ein sterkt varierande frekvens. Modellane av kraftverka fungerte godt til det meste. Det er likevel rom for eit par forbetringar. Tubinmodellen treng nokre endringar for å virke i stengt tilstand. Det bør og vurderast å implementere nye modellar for generator og regulator. Generatoren er nok ikkje nøyaktig nok til å simulere FRT-problem og modellen til spenningsregulatoren ikkje ser ut til å verke som den skal. Meir måledata frå FRT-testar bør og hentast inn før ein trekker endelige konklusjonar.

Abstract

The energy production in Europe is heading towards a green shift. The energy produced be renewable sources such as solar and wind are increasing day by day. This does however lead to a few issues. The energy produced by wind and solar power does not contribute in stabilizing the grid frequency as well as energy produced by fossil fuels. If this is not compensated for the grid frequency might experience larger variations than today, which is not desirable. From a hydro power perspective this fluctuating frequency will travel from the grid through the generator and turbine and it may cause pressure pulses in the conduit system in the power plant. In this thesis Bogna power plant will be investigated to check if and to what degree variations in the grid frequency will influence the power plant.

As a part of the green shift there has been a large development of small hydro power plants in Norway. With the introduction of new grid codes that are supposed to unite the Norwegian standards to the rest of Europe the has been asked question of how well the small hydro power plants are able to handle small voltage deviations. In cooperation with SINTEF Bruvollelva power plant has been tested for such deviations.

Both power plant has been modeled and simulation. The method used are the Method of Characteristics described by *Wylie & Streeter*. The method is implemented in the graphical programming package *Simulink* which is based on MATLAB. All the typical elements in a hydro power plant are implemented from the upper and lower reservoirs via the conduits, creek intakes and surge arrangements to the generator and runner. The turbine and generator are governed with classical PI-governors. In addition to this simple pressure measurements are preformed on Bruvollelva.

The last field measurement on Bruvollelva yielded quite unexpected results. The pressure measurements showed something that reassembles a full water hammer course. This was attempted replicated in the simulations without success. The simulated values presented a much smaller pressure increase.

The simulations of Bogna showed that the power plant will not be influenced to a large extent by a strongly varying frequency. The implemented models worked satisfactory for most simulation. There are however still room for a couple of improvements. The implementation of the turbine does not handle the closed state and tend to crash when the guide vane opening gets very small. The author does also question if the model of the generator is satisfactory accurate to model FRT-problems properly. In addition to this the two governors should be implement differently since they do not seem to work properly. More data from measurements should also be collected before arriving at a conclusion.

Table of Contents

List of Figures

List of symbols

Symbol	Description	Unit
A	The area of the pipe section	m^2
a	Pressure propagation speed	$\mathrm{m\,s}^{-1}$
B	Pipe characteristic impedance, a/gA	$\mathrm{s\,m}^{-2}$
c	The velocity of the servo motor	$\mathrm{m\,s}^{-1}$
C_P	MOC for the positive characteristic slope	m
C_M	MOC variable for the negative characteristic slope	m
D	Pipe diameter	m
E	Generator output voltage	V
f	Darcy friction factor	-
f_g	Grid frequency	Hz
g	The gravitational constant	$\mathrm{m\,s}^{-2}$
H	Piezometric head	m
h_f	Total head loss	m
$h_{f,q}$	Stationary head loss	m
$h_{f,u}$	Unsteady head loss	m
I	The hydraulic inertia in front of and in the turbine	$\mathrm{kg/m}^4$
J	The rotating mass for the turbine and generator combined	kgm^2
k_t	Transient friction constant	-
m_d	Generator torque dampening factor	-
m_s	The dimensionless starting torque of the runner	-
P	Produced power	W

Symbol	Description	Unit
Q	The volume flow travelling through the system	$\mathrm{m^3/s}$
q	Reduced flow through the runner, Q/Q_R	-
R	Pipe resistance coefficient, $f\Delta x/(2gDA^2)$	$\mathrm{s^2/m^5}$
r	Turbine radius	m
R_c	Loss factor for the runner inlet	-
R_d	Draft tube loss factor of the runner	-
R_f	Viscous loss factor of the runner	-
R_m	Mechanical loss factor of the runner	-
s	The self governing parameter of the turbine	$\mathrm{m^2}$
T	Torque of the turbine or generator	N m
T_a	The machine time constant	s
T_d	The integration time constant of the regulator	s
T_{dg}	The integration time of the voltage governor	s
T_K	The time constant of the servo motor	s
t_R	Rated specific torque of the runner	$\mathrm{m^2\,s^{-1}}$
t_s	The specific starting torque of the turbine	$\mathrm{m^2\,s^{-1}}$
T_{wt}	The turbine inertia time constant	s

Greek symbols

Symbol	Description	Unit
α_1	The guide vane angle	-
β_1	The turbine blade inlet angle	-
β_2	The turbine blade outlet angle	-
$\cos\varphi$	The power factor of the electrical grid	-
δ_t	The transient speed droop of the turbine	-
δ_{bg}	Permanent voltage droop	-
δ_b	The permanent speed droop of the turbine	-
δ_{tg}	Transient voltage droop of the generator?	-
η	Efficiency	-
κ	Guide vane opening	-
$k\phi$	The generator flux density	$\mathrm{km\,s^{-2}\,A^{-1}}$
ω	The rotational speed of the turbine	$\mathrm{s^{-1}}$
ψ	Machine constant, pressure number	-
ρ	The density of a fluid	$\mathrm{kg/m^3}$
σ	The dimensionless self governing parameter of the runner	-
ξ	Machine constant, spin at the inlet of the runner	-

Subscrips

Term	Description
1	Values at the inlet of the turbine
2	Values at the outlet of the turbine
g	Subscript denoting values for the generator
L	Denotes the segment to the left of the middle segment in question
P	Denotes the middle segment
R	Denotes the segment to the right of the middle segment in question
res	Subscript denotes values at the reservoir
t	Subscript for denoting turbine values

Abbreviations

Term	Description
BEP	Best Efficiency Point
CFD	Computational Fluid Dynamics
DAC	Digital to analogue converter
FRT	Fault Ride Through
MOC	Method Of Characteristics
mWc	Meters of water column
ODE	Ordinary Differential Equation
PDE	Partial Differential Equation

1 | Introduction

The European power grid is heading towards a green shift. The amount of electrical energy produced by renewable energy sources is increasing day by day and especially wind and solar power have had a large increase in power production over the previous years. There are however a couple of negative consequences with the increasing amount of solar and wind power in the energy mix. To this date no ways to control the sun or the wind. The produced amount of energy will have large variations from day to day and from hour to hour which in turn may cause the grid frequency to vary significantly if not balanced with a change in production from other sources. In 2014 Solvang et al. investigated the possibility of developing more hydro power in Norway by building new power plants and upgrade existing ones. The main purpose behind this report were to check if the Norwegian power plant were able to balance the European power market by selling Norwegian electricity when the demand and price were high in the rest of Europe and the buy cheap power in low-demand times of the day for use in pumped storage facilities [18]. Due to the fact that a photoelectric panel will produce a direct current and voltage instead of the alternating current and voltage we find of the power grid the solar power plant will not help in any way with stabilizing the grid frequency to 50 Hz. The same goes for the wind turbines which are mostly fitted with asynchronous generators that does not produce power with a frequency of 50 Hz. The increasing amount of solar and wind power will therefore most likely make the stabilization of the grid frequency harder.

To keep the grid frequency under control during the rapidly changing production from wind and solar power we need power plants that are quickly governed and can change production set point at short notice. Hydro power plants with large reservoirs such as Bogna are excellent for this purpose. There are however uncertainties how the excising plant with today's layout can handle the large deviations in frequency that may be caused by the large penetration of new renewables. One of the two major topics of this thesis is how a rapidly changing frequency is influencing the U-tube oscillations of this power plant.

The amount of energy produced by small hydro power plants has also increased considerably in Norway the ten previous years (from 277 in 2000 to 704 today according to NVE). In Norway a small hydro power plant is by definition a power plant with installed power less than 10 MW. Most of these are run-of-the-river power plants. The energy produced by these power plants is highly dependent on the inflow which typically is when the general demand for power is low such as in the snow melting season or the autumn. It might therefore be that in the foreseeable future periods where the whole Norwegian power demand is supplied by non-governable renewable energy sources such as small hydro power plants, solar power and wind power. In such a scenario it is highly undesirable that the small hydro power plants active will disconnect at the event of a

minor voltage deviations on the power grid. This is mainly the responsibility of the generator. The generators ability to handle such deviations are called the Fault Ride Through (FRT) properties and it is defined in the grid codes for the Norwegian power grid [19]. For larger power plants these are well defined and documented but for small hydro power plants these have not been properly defined until recent years. The FRT properties and what test that is used to find them are more thoroughly explained in chapter 2.

1.1 The power plants

This thesis will mainly focus on the two following power plants. Bruvollelva power plant is a small hydro power plant with an installed power 3.9 MW. The second power plant is Bogna power plant which is a rather large hydro power plant in comparison. Both are located along Snåsavatnet in Nord-Trøndelag. A short description of both plants follows below.

1.1.1 Bruvollelva

Bruvollelva power plant is a small hydro power plant located at the north bank of Snåsavatnet in Nord Trøndelag. The installed power is 3.85 MW. The runner in the power plant is a horizontal Francis runner with a maximum capacity of 3.9 $\mathrm{m^3\!/\!s}$ and a rated rotational speed of 750 rotations per minute. The effective head and thereby the design head of the runner is assumed to be in the magnitude of 110 Meters of water column (mWc).

The conduits system for the power plant is very simple and consists of a single straight pipeline where the pipeline at one point needs to cross the river. The pipeline mostly consist of reinforced fibreglass pipes but at the river crossing iron is used to avoid any further reinforcements of the pipeline. Almost everything of the 1100 meters of fibreglass sections are buried in the ground except the entrance to the power plant. The total length of the pipeline is 1350 meter where 250 meter consists of iron [17].

The power plant has no tail race tunnel to consider. It is therefore assumed that the water that exits the draft tube goes straight into the lower reservoir. The propagation speeds for the fibreglass and iron pipe section are assumed tos correspondingly to 800 and 1400 $\mathrm{m/s}$. This is done to keep the amount of cells to a reasonable number and to avoid unnecessary small time steps (the simulation time step is dependent on the cell length).

1.1.2 Bogna

Bogna power plant is located just a couple of kilometres south of Bruvollelva. With an upper reservoir at Bangsjø and a lower reservoir at Snåsavatnet which are both quite large this power plant is ideal for balancing the Norwegian power grid. A rough sketch of the power plant layout is
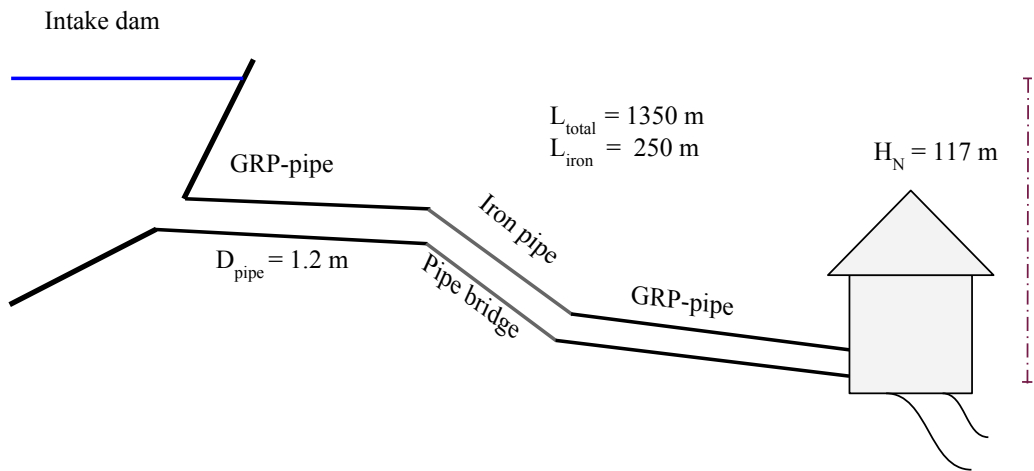
Figure 1.1: Sketch of Bruvollelva power plant

shown in appendix C. The power plant has one installed vertical Francis turbine with an maximum power of 55 MW. The net head from Bangsjø to Snåsavatnet is between 290 and 280 meters depending on the water level in Bangsjø. The design head for the turbine is 270 mWc and the design flow is 16.9 m^3/s. The rated rotational speed of the runner is set to 500 rotations per minute.

The power plant has a rather simple layout with one single turbine and corresponding penstock as well as long head and tail race tunnels. The surge shaft of the power plant are placed at the end of the head race tunnel. The surge shaft has a rather untraditional layout compared to most other power plants. The down-surges will however be effectively dampened out by the increasing area in the bottom of the shaft. The surge shaft is shown in the sketch in figure 1.2. Please be aware that the dimensions in the figure do not correspond to the actual scale.
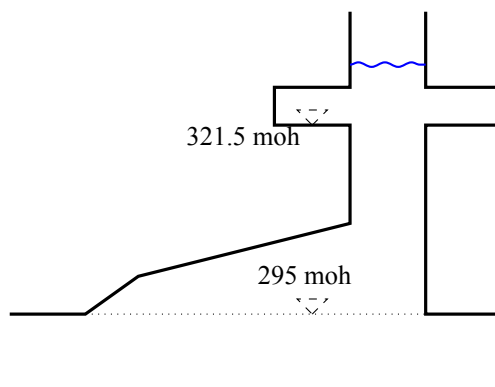
Figure 1.2: A sketch of the surge shaft

Both the head race tunnel and the tail race tunnel is quite long. With a total tunnel length of almost 6 km (the head race tunnel is approximately 3.5 km and the tail race approx. 2.4 km) the surges

in both tunnels can be quite large if not handled properly. Here both the surge chamber and the creek intake play important roles in handling and reducing the water hammer transients.

"Norwegian hydropower for large-scale electricity balancing needs" proposes to expand the power plant from the installed 55 MW to a 250 MW pumped hydro storage facility. The original plan were to implement a model for as well as the existing layout. The pump turbine model did however take a lot longer time than expected to implement with the consequence that there were not enough time to model the proposed layout of Bogna.

1.2   Previous work

There has been written numerous articles and theses written of both simulations of hydro power plants and other water hammer phenomenon. In the article by Zhao and Ghidaoui different types of water hammer flows is simulated using different numerical schemes [23]. The schemes investigated are the method of characteristics as well as a general finite volume scheme (the Godunov scheme with a slope limiter). A scheme based on the finite difference method are also considered. This article also compares the simulated values with theoretical and experimental data.

A good approximation of the friction loss in the pipes and junctions are vital to get an accurate result. The classical steady state friction model is not very good at handling large pressure surges and tend to underestimate the dampening of these. A transient or unsteady friction model is therefore needed to model this more accurate. An unsteady friction model is also taken into account in the article "Simulation of transient flow in hydroelectric power plants using unsteady friction". Different unsteady friction model are thoroughly investigated in the PhD thesis by Storli who also compared the results of the models with experimental data [20]. The original plan were to implement one of these models in the simulations here but because of lack of time the simpler model proposed in "Some remarks on the momentum equation for fast transients" was chosen and implemented with satisfactory results [2, 6].

More specialized simulations of hydro power plants are also thoroughly investigated in previous papers and articles. Transient behavior of the power plant Janjce is described in the article "Numerical simulations of hydraulic transients in hydropower plant Jajce II". Here a MOC scheme coupled with a unsteady friction loss approximation is utilized to model the behavior of the power plant. In the master thesis by Haugen the MOC method for the conduits and the surge tank in the power plant *Driva* is coupled with the turbine model by Nielsen. In this thesis the generators in the power plant is modelled as well. This thesis does however lack a model for the transient friction loss. A pumped storage facility is modelled in the article from American Society of Civil Engineers. This article compares different results obtained when modelling the water way both with and without considering the elasticity of the water [1]. A turbine model is not considered here though. Pumped storage is also a topic in "Simultaneous transient operation of a high head hydro power plant and a storage pumping station in the same hydraulic scheme" [3]. This is however an experimental study of a power plant with two separate Francis turbine and two separate

pumps with a rather unusual layout. Different load rejection cases were tested with both turbines and pumps in operation simultaneously. The experimental results were than compared to different simulation results where both CFD and MOC methods were utilized.

There are to the author's knowledge no simulations of FRT properties that incorporates the dynamics of the conduit system and the turbine. There has been done simulations that focuses on the generator and the transformer. The turbine torque in these simulations are often considered to be constant throughout the FRT scenario. This thesis will show that a constant turbine torque are rarely the case for such a case.

[**This page is intentionally left blank**]

2 | Testing of FRT properties

2.1 Fault ride trough properties

The fault ride through properties of a power plant is a label of how well a power plant copes with minor errors on the power grid. To satisfy the conditions stated in *FIKS* a hydro power plant should be able to handle grid voltage deviations less or equal to the error shown in figure 2.1 if connected to a grid with a nominal voltage of less than 220 kV [19].
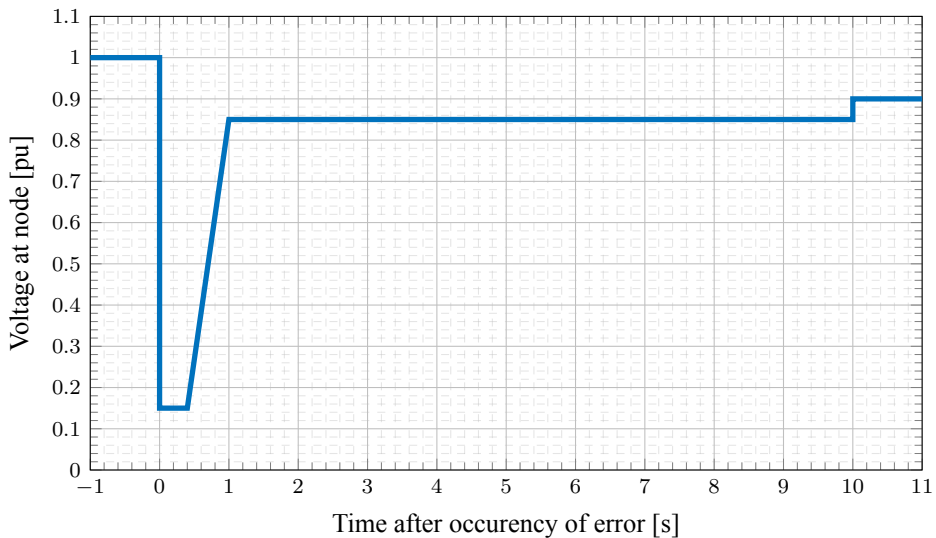
Figure 2.1: The Fault Ride Through curve defined by *FIKS*

If an error does not pass below the blue line in figure 2.1 the generator is supposed no to lose synchronization and keep on producing power during the voltage deviation. If the error crosses the blue line the generator is allowed to disconnect. It is however unclear how the dynamics in the runner and the conduits will behave during such a scenario and if it will influence the generators ability to meet the demands in *FIKS*.

2.1.1 The DipLab

The DipLab is a mobile 22 kV lab designed for short circuit testing of various power production facilities. It consists of two containers where one of the containers contains 24 reactances. These

Figure 2.2: The DipLab [15]

are use to control the depth of the voltage dip. The equipment for controlling the length of the dip is located in the second container. All the equipment for preforming measurements are located in the second container as well [15].

The reactances in the first container are used to produce the voltage dips such as the one shown in figure 2.1. They are also used to shield the grid from the voltage drop such that the disturbances produced by the DipLab is not propagating to the rest of the grid.

2.1.2 Testing for FRT properties

During the spring of 2016 there were preformed field measurements on Bruvollelva power plant in cooperation with SINTEF Energi. By utilizing the *DipLab* it was possible to lower the grid voltage in front of the generator and measure the response of the power plant. During this test the pressure in front of the runner was measured with a pressure transducer (Druck PTX1400, 0-100 bar a). The data from this sensor was logged with a data logger.

3 | Theory

This chapter will cover all the elements that are used to model Bruvollelva and Bogna power plant. The principles of how the conduit systems are modeled is shown in the chapter below with the basic pipe sections as the main building block but the junctions and surge arrangements are also thoroughly explained. The model of the turbine is explained in detail both in this chapter and the appendix. The generator is a somewhat simplified version of the one explained in *Electric machinery fundamentals* [5].

3.1 Pipes and surge arrangements

Water hammer and other transient phenomena is a closed fluid conduit are usually described using Allievi's equations. Using the Method Of Characteristics (MOC) described in *Fluid transients* this system of Partial Differential Equation (PDE)'s can be reduced to a system of two Ordinary Differential Equation (ODE)'s.

$$\frac{\partial H}{\partial x} + \frac{1}{gA}\frac{\partial Q}{\partial t} + h_f = 0, \tag{3.1.1a}$$

$$\frac{\partial H}{\partial t} + \frac{a^2}{gA}\frac{\partial Q}{\partial x} = 0. \tag{3.1.1b}$$

The MOC is a method used for reducing partial differential equations to ordinary differential equations. PDE's are hard to deal with and model efficiently. Therefore the Method Of Characteristics is used to reduce the PDE's to ODE's which are easier to deal with. The equations (3.1.1b) and (3.1.1a) are the continuity and momentum equations for one dimensional, slightly compressible problems. In (3.1.1) H piezometric head or the height different between the two points in question. Q is the the volume flow in the pipe. These are solved for along the characteristics lines of the equation system which is found by the Method Of Characteristics over the desired interval of time. A and a represents the area and pressure propagation speed for the pipe section. g is the gravitational constant and h_f is the head loss obtained through the pipe and may be computed using equation (3.1.2). The head loss may be split into two parts, the steady state head loss, $h_{f,q}$, and the transient head loss, $h_{f,u}$ as done in formula (3.1.2).

$$h_f = h_{f,q} + h_{f,u} = f\frac{Q|Q|}{2gDA^2} + \frac{k_t}{gA}\left(\frac{\partial Q}{\partial t} - a\frac{\partial Q}{\partial x}\right) \tag{3.1.2}$$
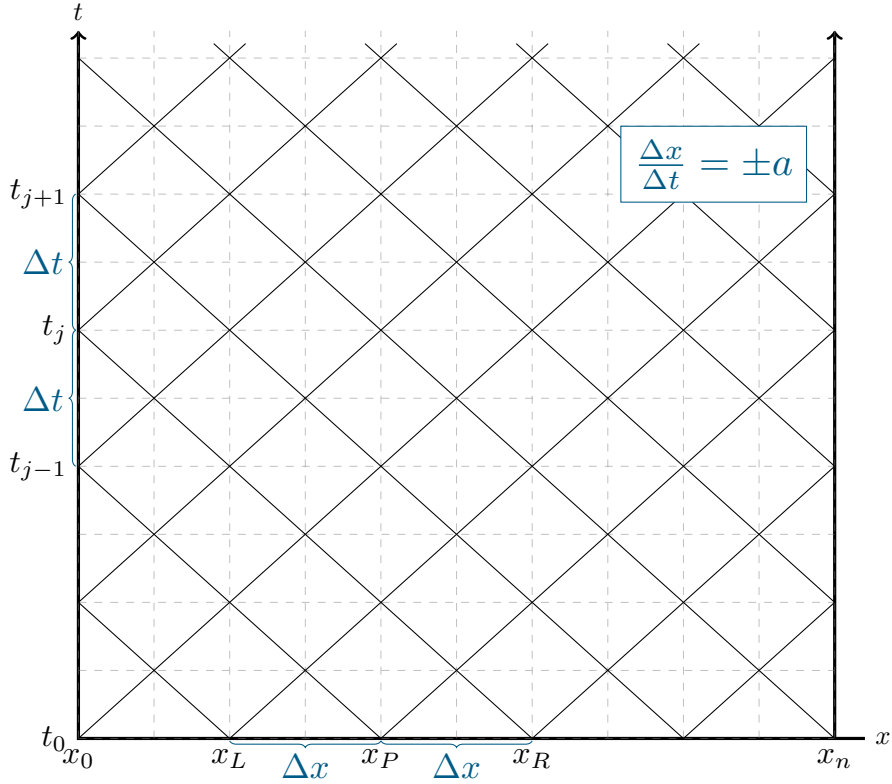
Figure 3.1: Example of a characteristic grid

Here f is the Darcy-Weisbach friction factor. This is found for each iteration by using the Håland's formula (the Colebrook relation was hard to implement and very computationally demanding) [4, p. 358]. The unsteady head loss are approximated by using a one coefficient model proposed in "A Review of Water Hammer Theory and Practice" and "Some remarks on the momentum equation for fast transients" [2, 6]. This is, due to the extra demand for computational power, only used for the simulations of Bruvollelva power plant. By utilizing MOC on equations (3.1.1) the system of equations may be reduced to:

$$\frac{1}{a}\frac{d\,H}{dt} + \frac{1}{gA}\frac{d\,Q}{dt} + h_f = 0, \qquad \frac{dx}{dt} = a \tag{3.1.3a}$$

$$-\frac{1}{a}\frac{d\,H}{dt} + \frac{1}{gA}\frac{d\,Q}{dt} + h_f = 0, \qquad \frac{dx}{dt} = -a. \tag{3.1.3b}$$

The system of equations is now reduced from a system of two PDE's to a system of two ODE's. By integrating the two ODE's from left to right one can obtain a system of equations one may solve in a programming language suited for this (such as Simulink used in this report). The completed equations is shown in equations (3.1.3).

By using the notation introduced by Wylie and Streeter in *Fluid transients* the final system of

equations may be stated as equations along the positive characteristic slope, C^+, or the negative characteristic slope, C^-:

$$C^+ : \quad H_P = H_L - B(Q_P - Q_L) - RQ_L|Q_L| - \frac{k_t}{gA}\left(\frac{\Delta Q_P}{\Delta t} - a\frac{Q_P - Q_L}{\Delta x}\right), \quad (3.1.4a)$$

$$C^- : \quad H_P = H_R + B(Q_P - Q_R) + RQ_R|Q_R| + \frac{k_t}{gA}\left(\frac{\Delta Q_P}{\Delta t} - a\frac{Q_R - Q_P}{\Delta x}\right). \quad (3.1.4b)$$

Here B and R are the Allievi coefficient and the pipe resistance coefficient. ΔQ_P may be approximated as $Q_P^{n+1} - Q_P^n$, where n denotes the time step. The constant is a function of a and area of the specific pipe and may be calculated as: $B = a/gA$. The pipe resistance coefficient is calculated in a similar manner: $R = f\Delta x/(2gDA^2)$. By introducing another two variables, C_P and C_M, the head can be calculated:

$$H_P = \frac{C_P + C_M}{2}. \quad (3.1.5)$$

With the head known for each nodal point, one of the two following equation may be used to calculate the flow in the nodal points:

$$C^+ : \quad Q_P = \frac{C_P - H_P}{B}, \quad (3.1.6a)$$

$$C^- : \quad Q_P = \frac{H_P - C_M}{B}. \quad (3.1.6b)$$

The variables C_P and C_M can be calculated by using known values from the previous time step:

$$C_P = H_L + BQ_L - RQ_L|Q_L|, \quad (3.1.7)$$

$$C_M = H_R - BQ_R + RQ_R|Q_R|. \quad (3.1.8)$$

3.1.1 Inlets, junctions and surge arrangements

Upper reservoir and inlet

The inlet is modeled as a pipe section with constant reservoir head. By using the notation introduced in section 3.1 the flow in the inlet section may be computed by the negative characteristic, C^-, and the fixed reservoir head.

$$Q_{res} = \frac{H_{res} - C_M}{B} \quad (3.1.9)$$
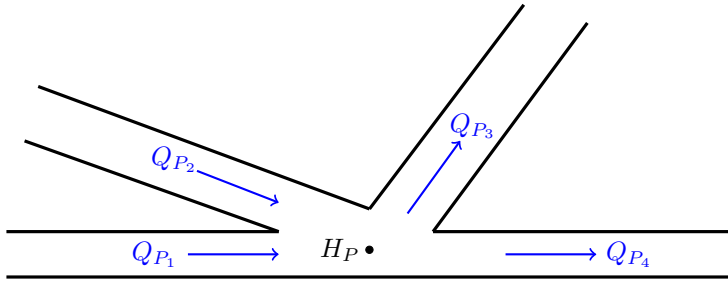
Figure 3.2: Illustration of a 4 port junction

Junctions

Sometimes the need to connect more than two pipe sections together arise. To do that correctly, a compatible model for junctions are needed. As for other parts of the power plant, the continuity equations also need to be fulfilled for the junction:

$$\sum_{p=1}^{n} Q_p = 0 \tag{3.1.10}$$

where *n* is the number of pipes connected to the junction. To solve this the head is assumed to be the same in all the section connected to the junction. The equation below is for a 4 port junction with two ports in and two ports out.

$$Q_{P_{1,NS}} = -\frac{H_P - C_{P_1}}{B_1} \tag{3.1.11a}$$

$$Q_{P_{2,NS}} = -\frac{H_P - C_{P_2}}{B_2} \tag{3.1.11b}$$

$$Q_{P_{3,1}} = \frac{H_P - C_{M_3}}{B_3} \tag{3.1.11c}$$

$$Q_{P_{4,1}} = \frac{H_P - C_{M_4}}{B_4} \tag{3.1.11d}$$

Surge shafts and creek intakes

In order to ensure satisfactory governability of power plant the pressure surges that occur at load changes as well as the surges that occur at start-up and shutdown has to be taken care of in a proper way. Another important aspect is that the power plant at start-up should not tear the string of water apart during the start-up procedure. To ensure that these criteria are fulfilled a surge chamber or a surge shaft often have to be installed. These often takes the form of an open surge shaft or a closed surge chamber. Here the surge shaft is modeled. A surge shaft or surge chamber effectively reduces the wave reflection time if placed close to the turbine. A smaller reflection time makes

ensures that the turbine may open and close the guide vanes over a reasonably amount of time (often between 2–10 seconds) without causing a massive pressure rise in front of the runner that might damage equipment.

The surge shaft model used for the simulations is also used in "Simulation of transient flow in hydroelectric power plants using unsteady friction" [14]. This model has lots of similarities with the junction described in the previous section and mathematically this is a junction with an accumulator element. The surge shaft is modeled with frictional losses in the standpipe but the losses in the accumulator is not considered. Since the hydraulic losses in the surge arrangements are rather small compared to the frictional losses in the head and tail race tunnel this is not considered a large simplification.

With losses in the standpipe considered the change in the surge shaft head may be expressed as:

$$\frac{dZ_S}{dt} = \frac{Q_{Sh}^{n+1} + Q_{Sh}^n}{2A_S}.$$
(3.1.12)

Together with the change in head the compatibility equations from the pipe systems has to be solved to find the flow going into the surge shaft. These are the same compatibility equations as described in section 3.1. In addition to these two the continuity equations are used to compute the surge shaft flow.

$$H_P - H_L + B \cdot (Q_{P_i} - Q_L) + R \cdot Q_L|Q_L| = 0$$
(3.1.13)

$$H_P - H_R - B \cdot (Q_{P_{i+1}} - Q_R) - R \cdot Q_R|Q_R| = 0$$
(3.1.14)

$$Q_{P_i} = Q_{Sh} + Q_{P_{i+1}}$$
(3.1.15)

In addition to this the head loss in the standpipe of surge shaft and the inertia in the surge shaft needs to be considered to get an accurate result.

$$\frac{L_{sh}}{gA_{sh}} \frac{dQ_{Sh}}{dt} = H_P - \underbrace{\frac{f_{sh}L_{sh}}{2gD_{sh}A_{sh}^2}}_{R_{sh}} Q_{Sh}|Q_{Sh}| - Z_{Sh}$$
(3.1.16)
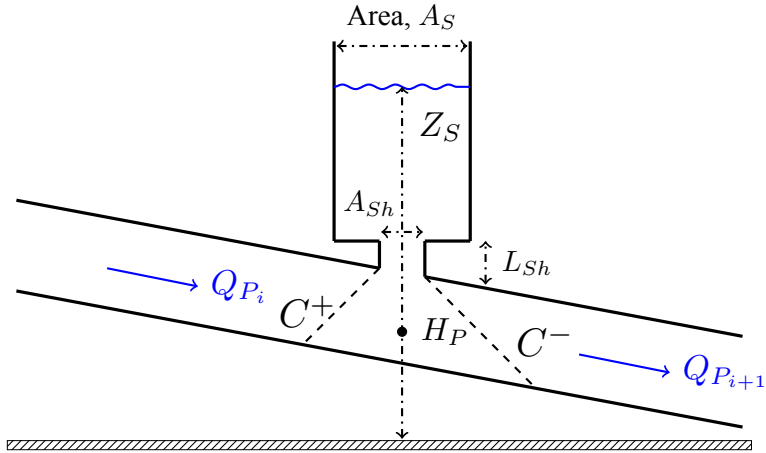
Figure 3.3: Illustration of a surge shaft

3.1.2 Approximation of the water hammer

To compare the check and compare the simulations some quick approximation formulas are shown here. This is approximations of equations (3.1.1). No hydraulic losses are considered in this approximation. The maximum pressure rise from the water hammer may be approximated as:

$$\Delta H_{WH} = -\frac{a\,\Delta Q}{g\,A} \tag{3.1.17}$$

This is only valid when the time span of the load rejection is less or equal than the reflection time of pressure wave. This is easily calculated: $T_R = {}^{2L}/a$ where L is the total length from the valve to the next free surface. For changes in volume flow that happens over a time span longer than T_R the following approximation has to be utilized:

$$\Delta H_{WH} = -2\frac{\Delta Q}{T_L}\frac{L}{g\,A} \tag{3.1.18}$$

where T_L represents the time span the volume flow is changed. For changes that takes place over a much larger time span than T_R the water hammer pressure becomes one half of the pressure rise computed with equation (3.1.18).

The approximation formulas are all taken from *Dynamisk Dimensjonering av Vannkraftverk* [11].

3.1.3 Modelling of the turbine

The model used for simulating the turbine is obtained from the PhD-thesis by Nielsen as well the articles dealing with the same topic [9, 10, 12, 13]. This model uses two ODE's, one for turbine momentum and one for the torque to describe the behavior of the turbine. To make the turbine

model compatible with conduits modeled on MOC form the classical turbine model has to be rewritten for this purpose. This is thoroughly explained in appendix B.3. The form described here is with dimensionless variables. The torque equation for the turbine is shown in equation (3.1.19).

$$T_a \frac{d\tilde{\omega}_t}{dt} = q(m_s - \psi\tilde{\omega}_t)\eta_h - R_m\tilde{\omega}_t^2 - \frac{T_G}{T_{t_R}} \tag{3.1.19}$$

The first terms one the right hand side of the equation, $q(m_s - \psi\tilde{\omega}_t) - R_m\tilde{\omega}_t^2$, describes the torque produced by the turbine while the second term describes the holding torque from the generator. The left hand side of the equation denotes the acceleration of the turbine. m_s describes the starting torque of the turbine. R_m is the mechanical loss coefficient of the turbine. ψ is the pressure number of the runner and in computed from the runner putlet peripheral velocity:

$$\psi = \frac{u_{2_R}^2}{gH_R} \tag{3.1.20}$$

The hydraulic efficiency is computed as a function of the mechanical losses and the incipient losses in the turbine. At operation away from Best Efficiency Point (BEP) there will always be some flow that will not enter the runner. This may be computed by relation (3.1.21).

$$q_c = \tilde{\omega}_t \left(\frac{1 + \dfrac{\tan\beta_{1_R}}{\tan\alpha_{1_R}}}{1 + \dfrac{\tan\beta_{1_R}}{\tan\alpha_1}} \right) \tag{3.1.21}$$

The total hydraulic losses in the runner may now be computed by equation (3.1.22) and the hydraulic efficiency found by equation (3.1.23).

$$\Delta h = R_f q^2 + (R_d + R_c)(q - q_c)^2 \tag{3.1.22}$$

$$\eta_h = 1 - \frac{\Delta h}{h} \tag{3.1.23}$$

The change of momentum through the runner may be described with an Ordinary Differential Equation (ODE) in the same manner as the change in torque. The change in momentum may be written on the form:

$$H_R T_{wt} \frac{dq}{dt} = HC - B_t Q_R q - H_R \frac{1}{1+\sigma} \left[\left(\frac{q}{\kappa}\right)^2 + \sigma\tilde{\omega}_t^2 \right]. \tag{3.1.24}$$

The momentum is multiplied with the rated head, H_R, to keep the same dimensions as in the characteristics scheme for the conduits. The available head is given by the pressure in pipe sections just before and just after the turbine element. The pressure term in equation (3.1.24) may be found as $HC = C_{P_L} - C_{M_R}$. The Allievi constant for the turbine, B_t, will now become the sum of the

Allievi constants in the neighbouring section, $B_t = B_L + B_R$.

In equation (3.1.24) the constant σ arises. This is the self governing parameter of the runner and describes how the runner affects the flow when operating away from BEP. This constant is purely dependent on the geometry of the runner but for simulation purposes this often becomes inaccurate. The model used in this thesis is based on the Euler turbine equations and because of deviations from the Euler design criteria the classical form of the self governing parameter will not work satisfactory. The self governing parameter is therefore calculated using the pressure number, ψ, and the hydraulic efficiency η_{h_R}:

$$\sigma = \frac{\eta_{h_R} - \psi}{\eta_{h_R} + \psi} \tag{3.1.25}$$

Other important parameters in the two turbine equations are the time constants, T_a and T_{wt}. T_{wt} is often hard to pinpoint but values in the magnitude of 0.1-0.2 seconds is often used. The machine time constant is easier to measure and for large hydraulic machines this time constant often takes a magnitude of 5-8 seconds. For smaller machines (such as the one in Bruvollelva power plant) the time constant often is in the magnitude of 1-2 seconds [11, p. 76].

3.2 Modelling of the generator

To convert the rotational energy to electrical energy a generator is needed. The generator is connected to the runner through the generator shaft where the shaft is a metal rod that is bolted to the runner at one end and to the generator rotor in the other end. The constantly changing magnetic fields between the rotor and the stator in the generator generates the generator voltage, E. The generator in both Bruvollelva and Bogna power plant is of the synchronous type. A model suited for the simulations done in this thesis is found in *Electric machinery fundamentals* [5]. The model implemented models the generator as a polar moment of inertia with a torque that is dependent on the electrical load of the generator.

The generator torque is primarily dependent on the angle between the magnetic fields in the rotor and the stator, δ. For modeling and simulation purposes this angle is described as a differential equation. The angle may be found as the difference between the grid angular velocity and the turbine angular frequency. This is described in equation (3.2.1).

$$\frac{d\delta}{dt} = \frac{P}{2}\omega_t - \omega_g \tag{3.2.1}$$

where $\omega_g = 2\pi f_g$. f_g is the frequency of the electrical grid. In Norway this is assumed to be relatively constant at 50 Hz. P is here the number of generator poles. The generator torque is now approximated as a sine function:

$$\frac{T_g}{T_{g_R}} = \frac{\sin \delta}{\sin \delta_R} \tag{3.2.2}$$

where T_{g_R} is the rated torque of the generator and δ_R is the corresponding angle to this torque. To model the torque of the generator correctly the change in rotor-stator angle has to be taken into account in the torque equation. When the rotor-stator angle changes an extra dampening torque will arise. This is added to the generator torque equation as a function of a dampening factor, m_d, and the change in rotor-stator angle, $d\delta/dt$ has to be added to equation (3.1.19). The new torque balance now will look like:

$$T_a \frac{d\tilde{\omega}_t}{dt} = q(m_s - \psi\tilde{\omega}_t)\eta_h - R_m\tilde{\omega}_t^2 - \left[T_g + m_d\frac{d\delta}{dt}\right]\frac{1}{T_{t_R}} \tag{3.2.3}$$

With all the mechanical elements of the generator in place the electrical elements of the generator may be found. The voltage and the current of the generator may be found as a function of the magnetic flux in the generator, $k\phi$:

$$E_g = k\phi\omega_g, \tag{3.2.4}$$

$$I_g = \frac{T_g}{k\phi\cos\varphi}. \tag{3.2.5}$$

The generator flux is controlled by the excitation system of the generator which in turn is controlled by the voltage governor (more information in sec. 3.3.2). This is done to keep the produced voltage at a reasonably stable level and with a frequency of 50 Hz. The $\cos\varphi$ is the power factor of the grid. It described how much of the electrical energy that may be used for practical applications. Of simplicity reasons φ is fixed to 0 in all simulations which means the power factor is set to 1. In words this means that all the mechanical energy is converted to electrical power. In order to meet the demands on the grid in terms of both frequency and voltage both the turbine and the generator needs governing. The governors used in this thesis are simple PI-governors, witch consists of mainly two parts. The first one is the **P**roportional part which makes sure that the governor responds to deviations away from the wanted set point in the governor. The **I**ntegral part then removes the steady state deviations that occur when the proportional part has done its governing.

In addition to the proportional and integral parts the frequency governor is equipped with a permanent speed droop element that is supposed to adjust the guide vane opening if the turbine rotational speed changes away from synchronous speed.

It is worth mentioning that only Bogna power plant is equipped with a frequency governor. Since Bruvollelva is defined as a mini hydro power plan *FIKS* does not require it to install a frequency governor. The frequency governor is therefore not taken into consideration in the model of Bruvollelva.

3.3 Governing of turbine

3.3.1 Frequency governor

The frequency of the turbine is often governed by a PI-governor. In most cases this is sufficient when the grid is considered to be stiff (the produced power does no affect the grid frequency). When operating in island mode a derivative term is often added to the governor to ensure a quick response if the grid frequency deviates from the wanted frequency. The derivative term can cause instabilities in the system if not used with care. This thesis will only examine issues connected to grid connections and the D-term in the governor will therefore be omitted.

The frequency governor used in this thesis takes the inertia of the servo motor of the guide vanes into account. It also takes into the account the permanent speed droop of the unit, δ_b.

$$\frac{d\kappa}{dt} = c, \qquad (3.3.1a)$$

$$\frac{dc}{dt} = \frac{1}{T_k}\left[\underbrace{-\frac{1}{\delta_t}\frac{1}{\omega_{t,ref}}\frac{d\omega_t}{dt}}_{P} + \underbrace{\frac{1}{\delta_t T_d}\frac{\omega_{t,ref} - \omega_t}{\omega_{t,ref}}}_{I} - \frac{\delta_b T_k + \delta_t T_d}{\delta_t T_d}\cdot c \right.$$

$$\left. - \frac{\delta_b}{\delta_t T_d}(\kappa_{ref} - \kappa) \right] \qquad (3.3.1b)$$

The parameters in equations(3.3.1) describes the following:

$\kappa\ -$ Guide vane opening of the runner

$c\ -$ Servo motor velocity

$\omega_t\ -$ Turbine speed of rotation

$\delta_t\ -$ Transient speed droop

$\delta_b\ -$ Permanent speed droop

$T_d\ -$ Integration time

$T_K\ -$ Servo motor time constant

This governor controls the speed of the runner by adjusting the guide vane opening. If the speed of the runner deviated from the wanted rotational velocity the governor responds by changing the guide vane opening.

3.3.2 Voltage governor

For the electrical grid to work properly the generator has to keep the voltage reasonably stable. The voltage output level is governed by adjusting the magnetization in the generator. This is

done via the generator voltage governor which is a PI-governor that works in the same way as the frequency governor. The voltage governor adjusts the magnetization $k\phi$ such that the output voltage E fits the wanted level for the grid. The equation that is implemented to model the voltage governor is shown below:

$$\frac{d(k\phi)}{dt} = -\frac{1}{\delta_{tg}}\frac{1}{E_{ref}}\frac{dE}{dt} + \frac{1}{\delta_{tg}T_{dg}}\frac{1}{E_{ref}}\left[E_{ref} - E + \frac{1}{\delta_{bg}}\frac{1}{I_{ref}}(I - I_{ref})\right] \qquad (3.3.2)$$

The parameters in equation (3.3.2) describes the following:

$k\phi$ – Generator flux density

E – Generator output voltage

I – Generator output current

δ_{tg} – Voltage transient droop

δ_{bg} – Voltage permanent droop

T_{dg} – The integration time of the voltage governor

[**This page is intentionally left blank**]

4 | Implementation of the model

All the theory described in the previous chapters are implemented in the MATLAB add-on Simulink and used to model the power plants. A short description of how this is done is given below.

4.1 Pipes in Simulink

The equations described in section 3.1 are implemented in Simulink and put together to model a whole pipe section. An example of how this is done is shown in figure 4.1.
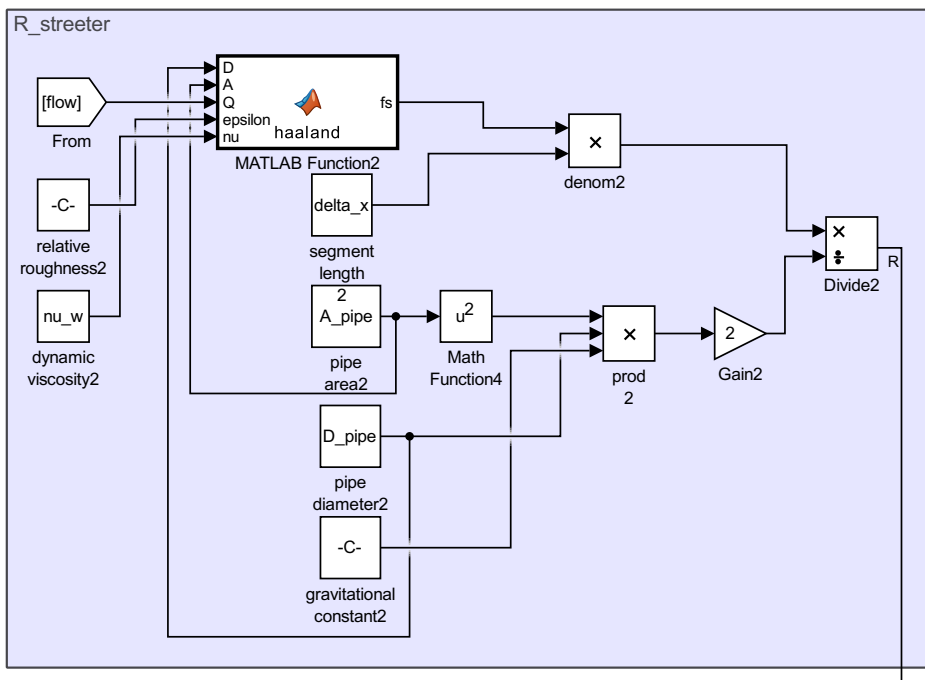
Figure 4.1: How the loss factor, R, is calculated in Simulink

The Darcy friction factor is calculated for each time step based on the flow in the pipe section. The MATLAB implementation of the formula is shown below. The friction factor is computed based on the volume flow in each pipe section from the previous iteration. This is done to make a faster simulation program as well to make the equation solver more robust against large transient.
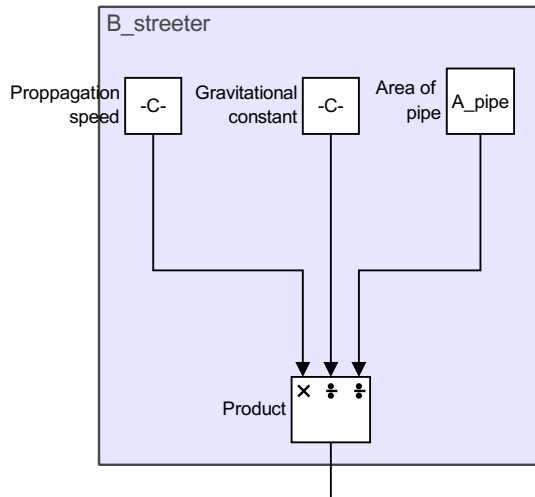
Figure 4.2: Computation of the Allievi constant for the pipe section

When the new values for the flow is used to find the new friction factor the simulations tends to crash when large transients occur.

The characteristic impedance of each pipe section is computed in a similar manner. Figure 4.2 shows how this is done for each pipe section in Simulink. With these constants in place the values for the characteristic lines, C_P and C_M may be computed and from those values the new flow and head for that given pipe section can be found. This then follows through for all the pipe segments.

```
function fs = haaland(D,A,Q,epsilon,nu)
fs = zeros(1);

%% Funtion that calculates the friction factor based on Colebrooks equation
%   Input
%   D       - diameter of pipe
%   epsilon - roughness of pipe wall
%   Q       - Volume flow in the pipe
%   nu      - Dynamic viscosity of water

Re = (abs(Q)*D)/(nu*A);

epsD = epsilon/D;

A = (epsD/3.7)^1.11; B = 6.9/Re;
f = -1.8*log10(A + B);

fs = 1/(f^2);

end
```

4.1.1 Calibration of the transient friction constant

To get a sensible value of the transient friction factor, k_t, the simulated values have to be calibrated against measured values. This is shown in figure 4.3. The dampening of the pressure waves corresponds best with a constant value of 0.25 and this value is used for the simulation described below. In the figure the guide vanes starts closing at 24 seconds and closes in about 4 seconds.

Due to the lack of measurements of rotational speed and volume flow in the turbine it is rather unclear what is happening during the second FRT test. It was not expected to measure a full water hammer so the simulations will here try to mimic the pressure rise measured during the test and try to explain what is happening with the whole system.

4.1.2 Junctions and surge arrangements

To be able to model long conduits with different cross sections and pressure propagation speeds, some junctions are needed. The junctions are in general special cases of a pipe section where the positive and the negative characteristics are separated from each other and the computations of flow are computed with the sum of the B's from the two neighboring sections. The same goes for the surge elements. These are junctions equipped with energy storage elements where the excess energy is stored in form of extra pressure in the surge elements. The energy storage elements are shown in figure 4.4.

This code block computes the surge height in the surge shaft based on the values in the neighboring pipe segments. The creek intake is modeled by the same code but with an extra input where the volume flow into the creek may be set externally.

4.2 Implementation of the turbine

The turbine equations described in section B.3 are also implemented in Simulink together with the governor equations described in section 3.3. These equations has to be solved simultaneously in order to get an stable system. In the simulations of Bruvollelva the frequency governor is omitted due to the fact that the power plants does not have one installed. How the dimensionless specific starting torque of the turbine, m_s is calculated is shown in figure 4.5.

The other turbine parameters such as the turbine rotational speed and the turbine head is calculated in other similar subroutines. The turbine characteristic impedance and the the available head of the turbine is calculated in the neighboring pipe sections.
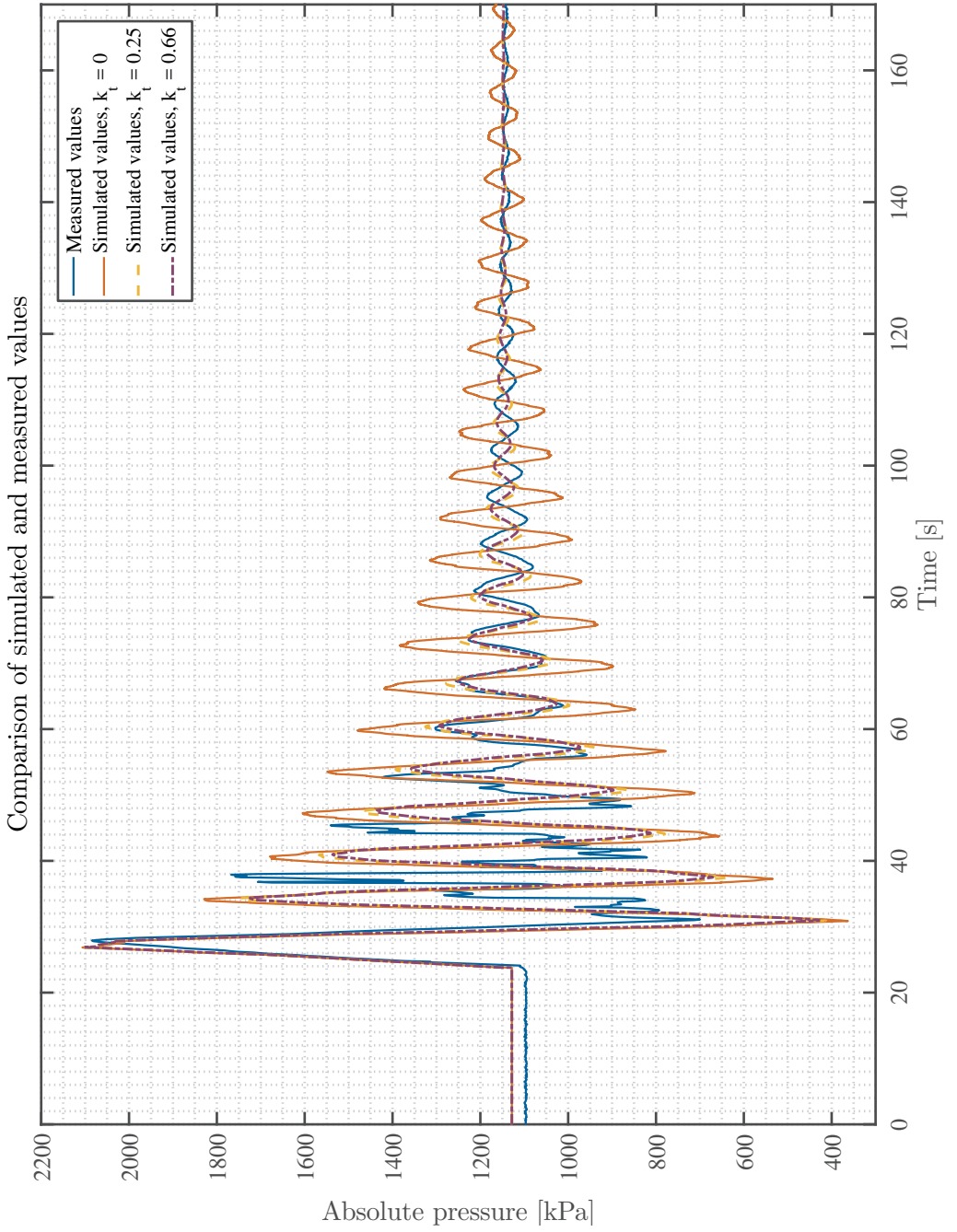
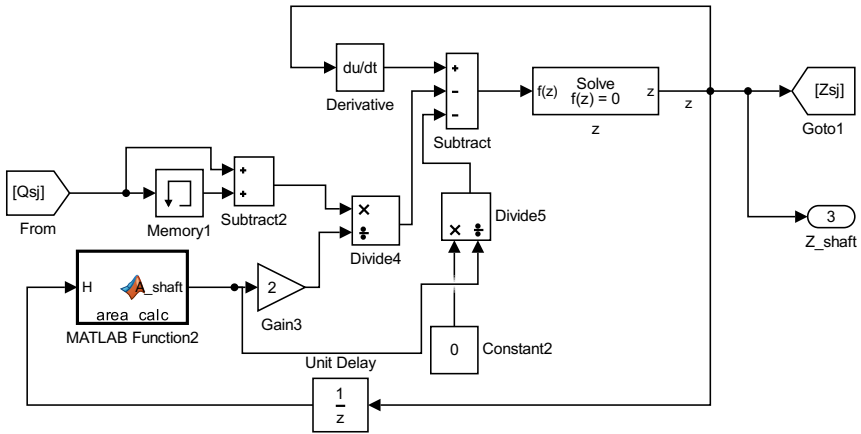Figure 4.3: Comparison between measured and simulated data in Bruvollelva power plant

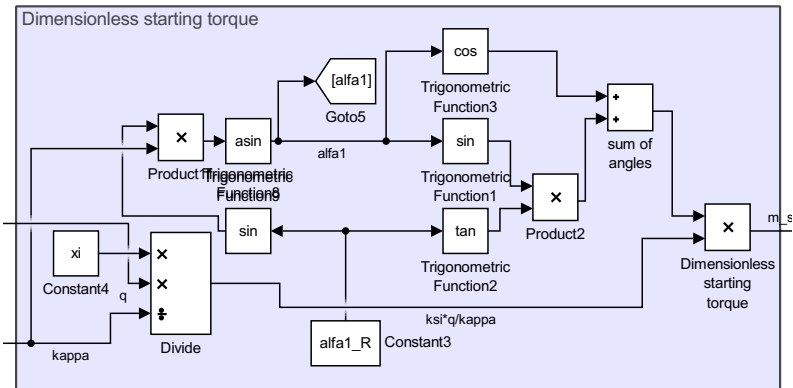Figure 4.4: The energy storage element in the surge shaft block

Figure 4.5: Calculation of the dimensionless starting torque

[**This page is intentionally left blank**]

5 | Bruvollelva kraftverk

5.1 Tests at Bruvollelva

There were preformed two sets of measurements at Bruvollelva power plant. This were done in cooperation with SINTEF which preformed their own test on the generator at the time. The test set-up were quite simple with one pressure transducer connect to a NI-USB 6211 DAC card which was connected to a laptop running and recording the measured data in LabVieW. The pressure transducer was connected to a distributor pipe just before the entrance of the spiral casing. The pressure transducer used for the measurements was a Druck PTX1400 with a range from 0 to 100 bar absolute pressure (the calibration documentation and the general uncertainty analysis for these measurements can be found in appendix G for the calibration documentation). With the uncertainty of the pressure calibrator being 0.008% and a maximum calibration uncertainty of 0.01338% the total systematic uncertainty of the measurements may be calculated using the approach stated in appendix G.1. The total systematic uncertainty of the measurements is calculated to can now be calculated:

$$f_{cal} = \sqrt{f_{ab}^2 + f_{reg}^2 + f_{pd}^2} = 0.05237\% \qquad (5.1.1)$$

which is what is used in the measurements presented below. This does not consider the random uncertainty of the measurements. This is hard to estimate with a sensor that is calibrated with static measurements. There are however several preformed with similar sensor on earlier occasions with good results. A simple sketch of the set up is displayed in figure 5.1. The measurement data is smoothed with a digital Savitzky–Golay filter before being plotted and added to the report. The unfiltered signal may be found in appendix D. The measurements done on grid voltage and generator current by SINTEF during the test may be found in appendix E

5.1.1 First Fault Ride Through test

In figure 5.3 the measured pressure in front of the turbine in shown. The parameters for the test were:

$$P - \quad 2 \text{ MW}$$
$$\kappa - \quad 0.6$$
$$\Delta E - \quad 0.12$$
$$\Delta t - \quad 0.5 \text{ s}$$
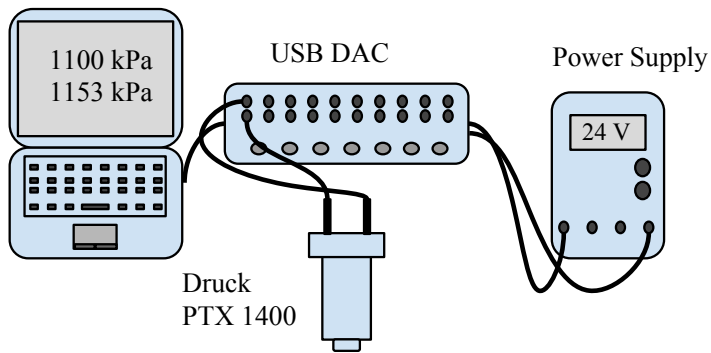
Figure 5.1: Illustration of the measurement set-up used in the Bruvollelva measurements

Illustration of the fault ride trough error [s]
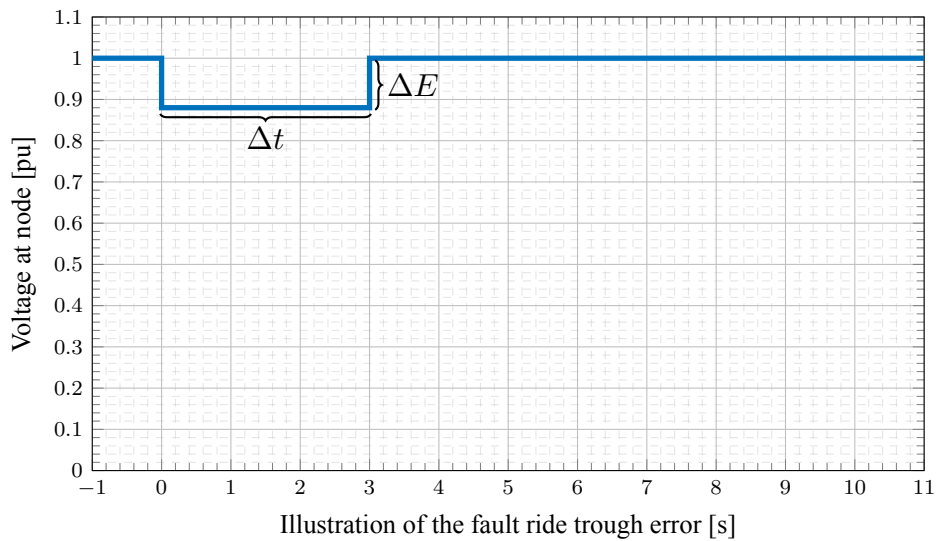
Figure 5.2: A graphical representation of the generator voltage during test two
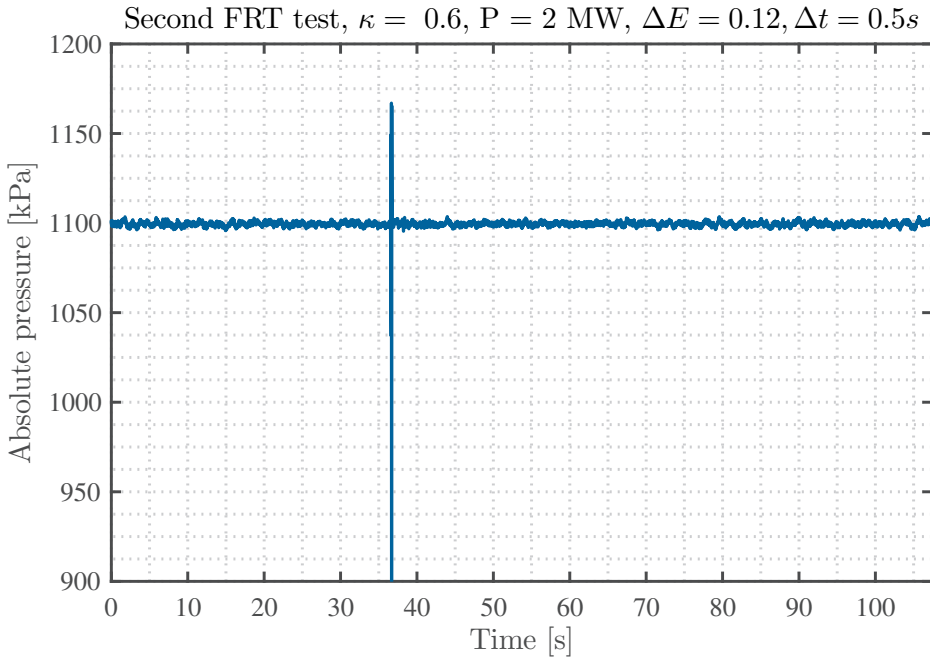
Figure 5.3: First FRT test preformed at Bruvollelva power plant

Here P is the produced power at the unit before the test were initiated, κ is the guide vane opening. ΔE and Δt is the change in node voltage and the duration of the voltage drop. The generator did not disconnect during this test. The measured voltage and current of the generator side is shown in figure E.1. After the test is done both the current and voltage returns to its original values.

5.1.2 Second Fault Ride Through test

Figure 5.4 shows the measured pressure in front of the turbine during the second FRT test. The parameters for the test were:

$P -$ 2 MW

$\kappa -$ 0.6

$\Delta E -$ 0.12

$\Delta t -$ 3.0 s

Here the generator disconnects and a classical water hammer scenario arises. In the figure the generator disconnects at approximately 24 seconds. The pressure in front of the turbine quickly rises after this. Due to the lack of measurements of the turbine rotational speed it is hard to pinpoint exactly what is happening here but the pressure rise corresponds well with the approximate pressure rise explained in section 3.1.2. The measured voltage and current on the generator side is
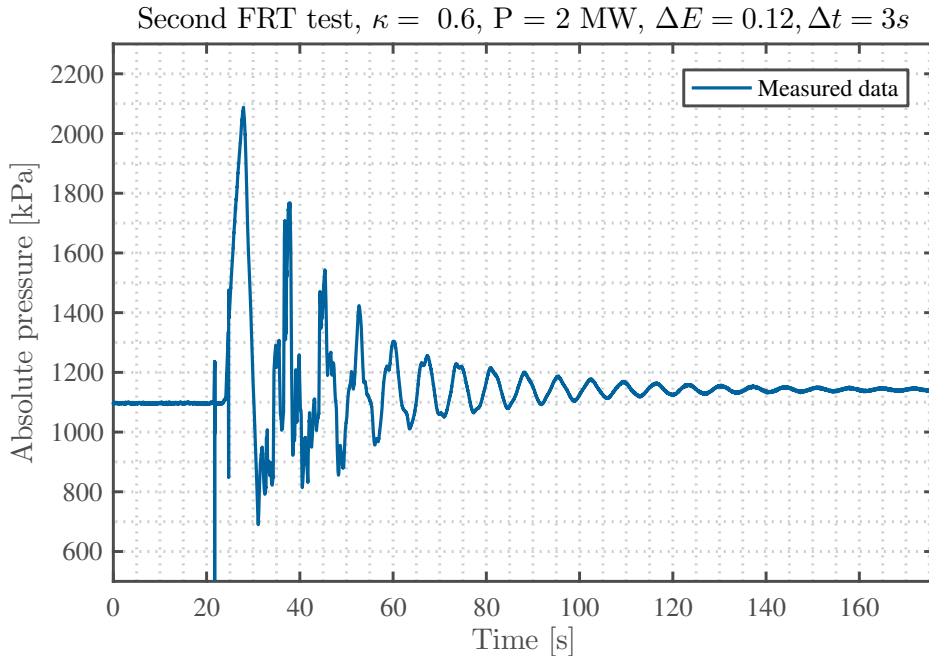
Figure 5.4: Measurements of water hammer phenomena at Bruvollelva Power plant

shown in figure E.2. The generator disconnects at approx. time 09:40.75 where the current drops to zero.

5.2 Simulation of Bruvollelva power plant

5.2.1 Simulations of Bruvollelva

Closing of guide vanes

In this simulation the guide vanes are closed over a time span of four seconds. As seen in figure 5.5 the guide vanes goes from an opening of 0.6 of the rated opening at 20 seconds to close to zero at 24 seconds. The pressure rise in the conduit system is shown in the second sub-figure here. The turbine and generator torque as well as the turbine speed is shown in the last sub-figure. The pressures shown in the middle figures are the pressures at the outlet of each section in figure 1.1. The subscripts *GRP* represents the outlet of the first fiberglass section, *iron* is the pressure at the outlet of the iron pipe section and *BT* is the pressure at the outlet of the second fiberglass section which assumed to be the pressure in front of the runner.
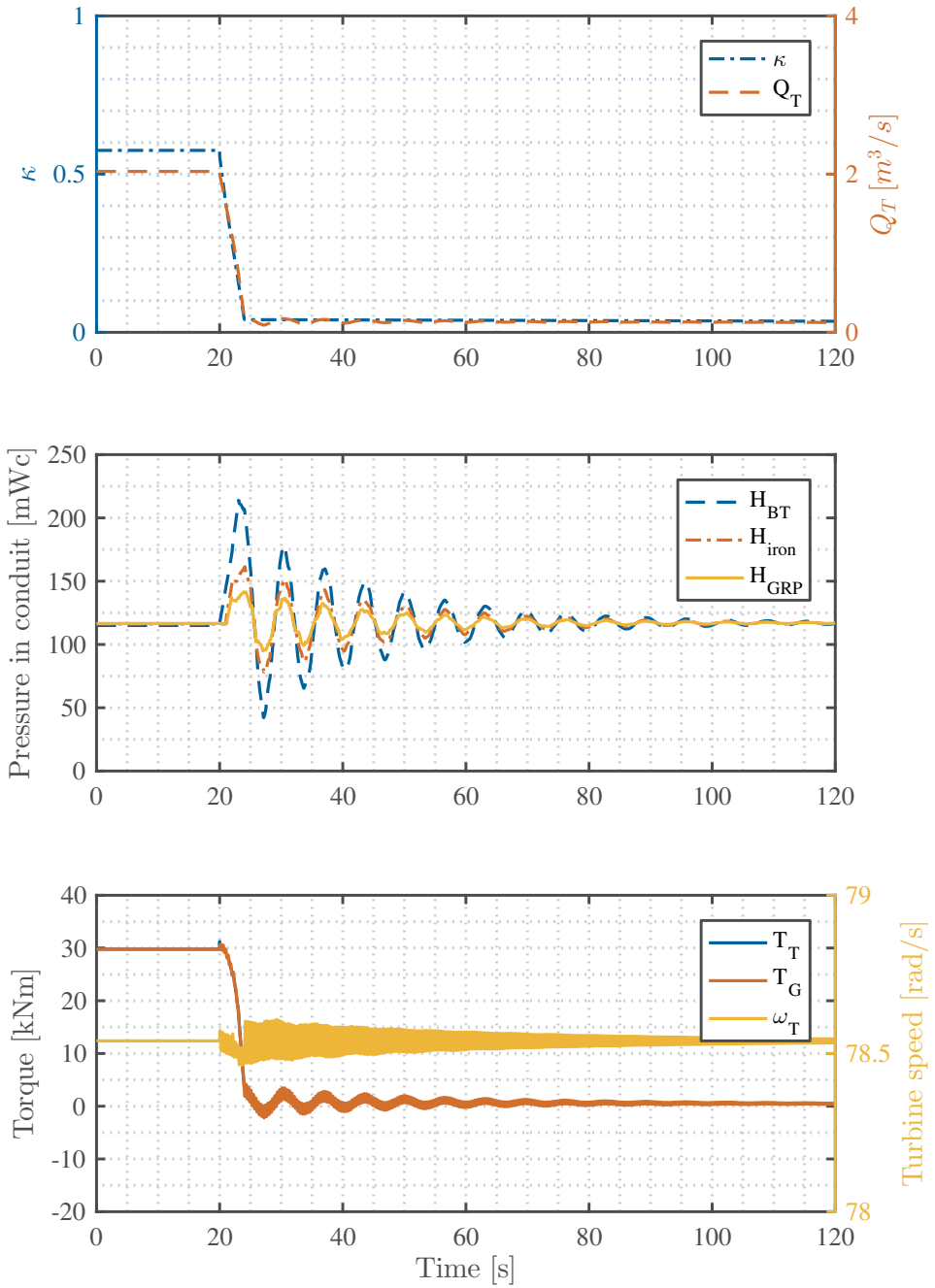
Figure 5.5: Behavior of the power plant when the guide vanes are closing over a time span of approx. 4 seconds

Sudden loss of generator torque

In this simulation the the generator is disconnected after 20 seconds. This is shown in the last sub-figure in figure 5.6. Over the next 7-8 seconds the turbine rotational speed (shown in the same sub-figure) doubles from the start point. The conduit pressure is shown in figure second sub-figure and the guide vane opening and the turbine flow in the uppermost sub-figure.

Disconnection of the generator combined with closing of the guide vanes

This simulation tries to combine the two cases described above in a sensible way. The generator will disconnect after 18 seconds as in simulation two before the safety system senses the increased turbine speed and closes the guide vanes in the same time span as described in simulation one. The result of this simulation is shown in figure 5.7.
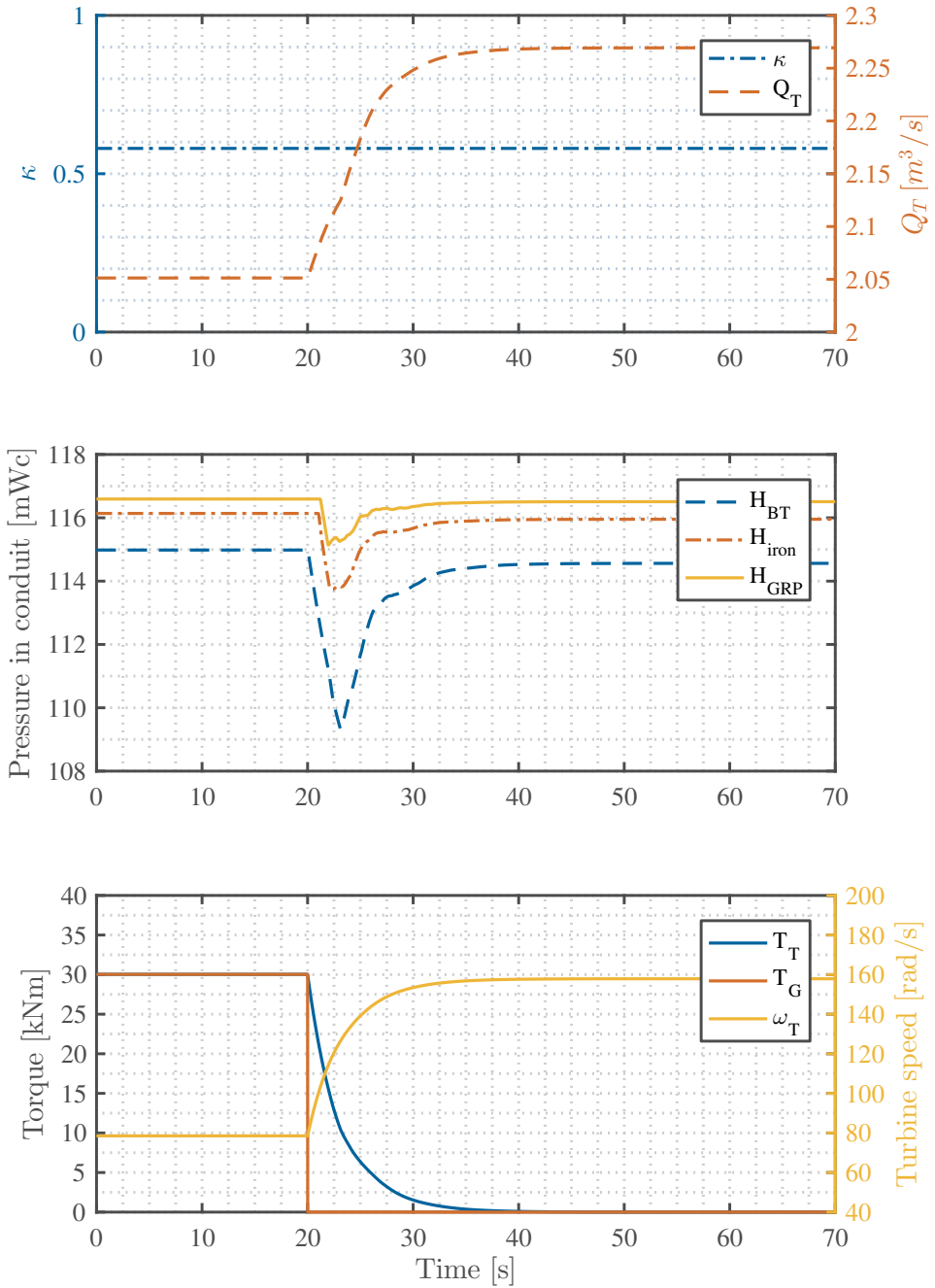
Figure 5.6: Behavior of the power plant when the generator disconnects suddenly
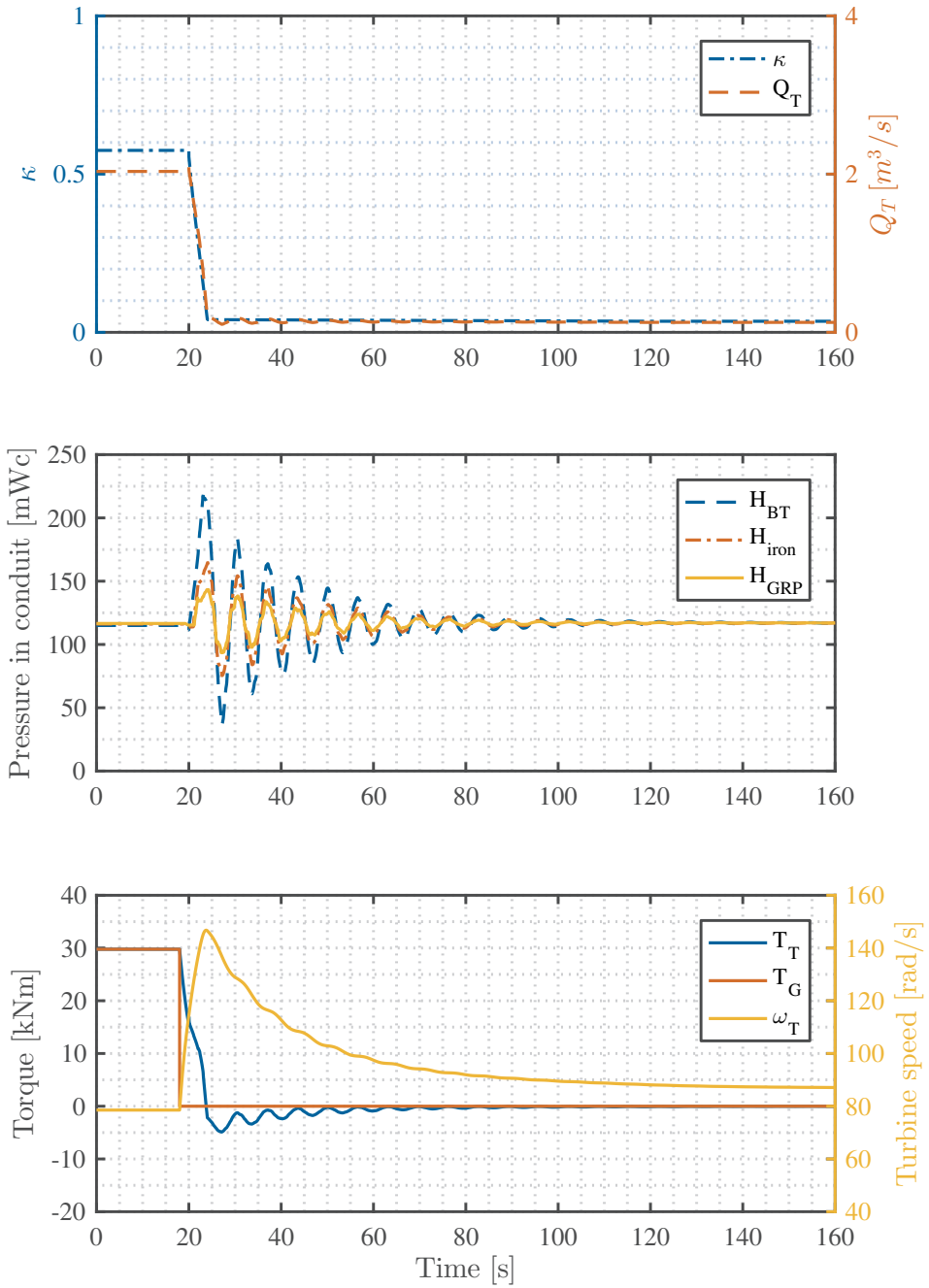
Figure 5.7: Behavior of the power plant with a disconnected generator with the guide vane closes in a Δt of 4 seconds

6 | Simulations of Bogna power plant

The first simulation done on Bogna is based on a measured drop of grid frequency and is used to make a reference of how the power plant will behave during varying frequency. The reference case is taken more or less from measurements, a real signal will be more noisy but the extremal points are taken and used as input for the simulations. The test cases are supposed to emulate more rapid changes of grid frequency that might come of more installation of renewables such as wind and solar power. These have asynchronous generators and will not contribute to grid stability in the same way as synchronous generators. The other two tests are supposed to simulate large changes in power input or output to the grid following by either a large loss of production (for instance if a Swedish nuclear power plant that suddenly drops off the grid) or a sudden disconnection of a large load (imagine a large aluminum plant somewhere in Norway). All simulation is done with the power plant running on approximately rated load and with a full upper reservoir making the head maximum of what is allowed.

6.1 Reference case

The result from this reference case is displayed in figures 6.3 and 6.4. The frequency input for this test is shown in figure 6.2. This frequency was measured at Grana on the first of January 2014. Bogna has probably experienced a couple of these over the last 15 years and this will therefore be used as a reference for the other simulations.

The behavior of the turbine during this case may be seen in figure 6.3 together with the generator torque. The behavior of the hydraulic elements, such as the water level in the creek intake and surge shaft are shown in the last sub-figure in figure 6.4. The produced power of the turbine is displayed in the same frame. The pressure both before the turbine and in the draft tube are shown in the middle figure and the guide vane opening as well as the volume flow trough the turbine are presented in the uppermost sub-figure.

6.2 Varying frequency with sudden loss of a large load

The input frequency for this case may be found in figure 6.5. The frequency here is supposed to show how the grid frequency might be influenced if a large load, such as a paper factory or an aluminum plant, suddenly for some reason is disconnected from the grid. Following the frequency spike the frequency is supposed to fluctuate around the reference frequency. The speed of the
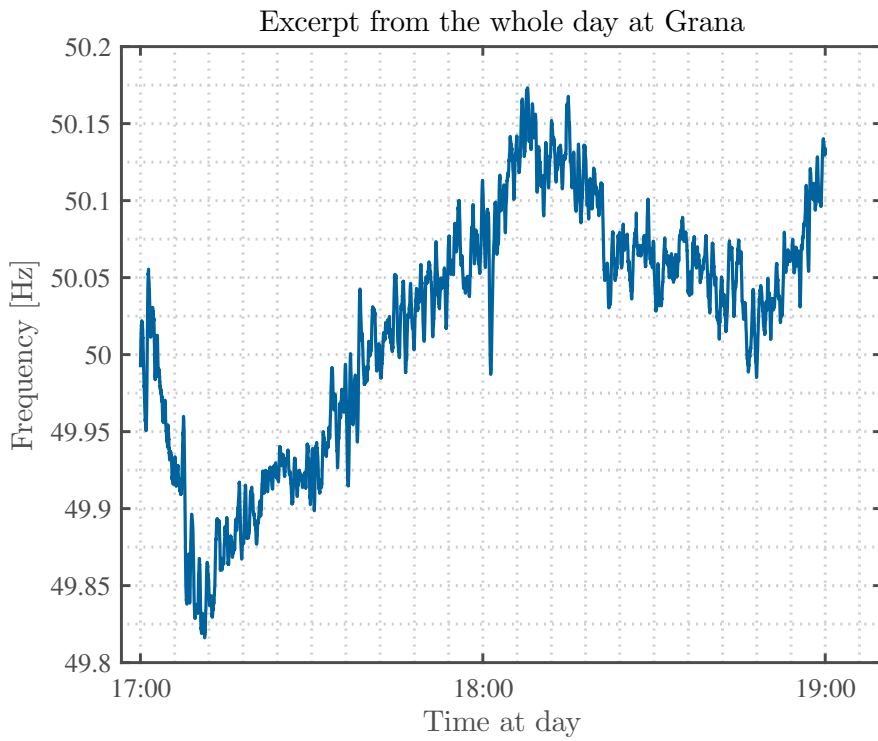
Figure 6.1: Measured frequency at Grana power plant on the first of January 2014
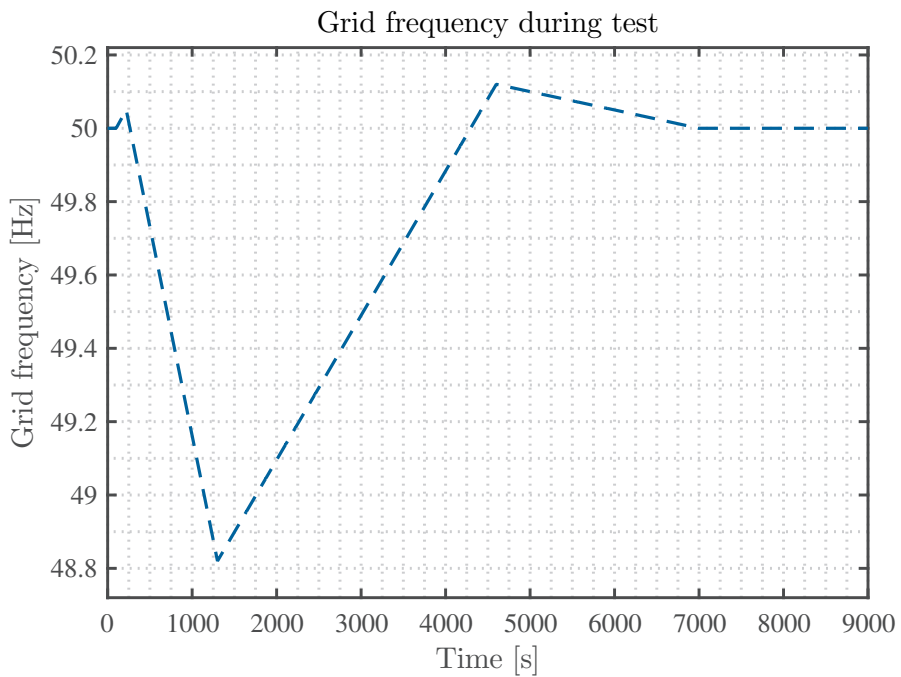
Figure 6.2: Input frequency for reference case
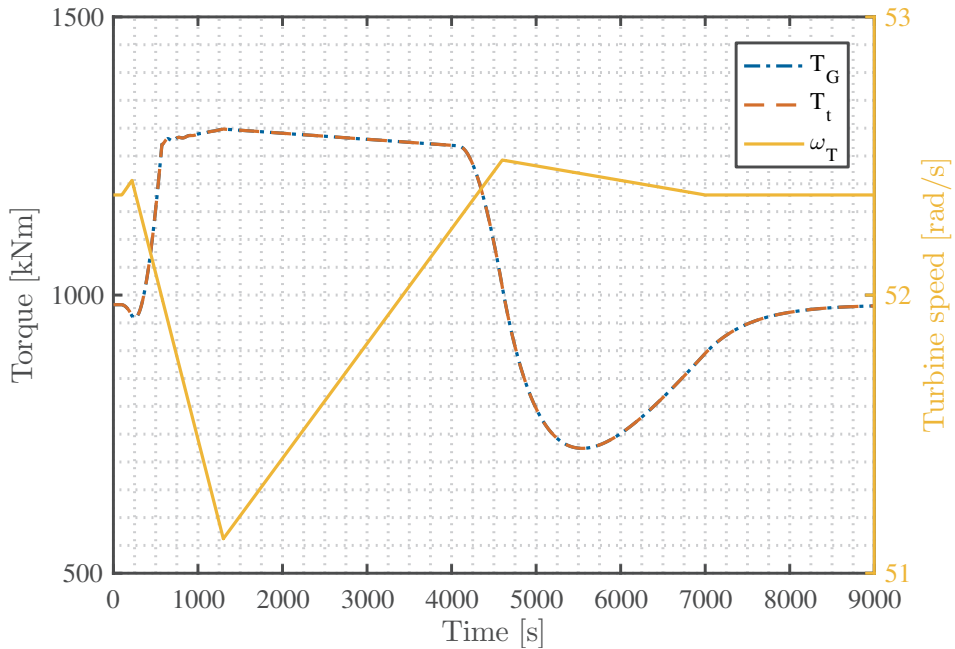
Figure 6.3: Turbine and generator behavior for reference case

runner with this input is displayed in figure 6.6 together with the turbine and generator torque. How the hydraulics in the system is behaving may be found in figure 6.7.

6.3 Varying frequency with a sudden loss of a large production facility

The input frequency for this case may be found in figure 6.8. This is more or less the inverted frequency of the one simulated in case 6.2. The results from the simulations of the turbine and the conduits system are shown in figure 6.9 and 6.10
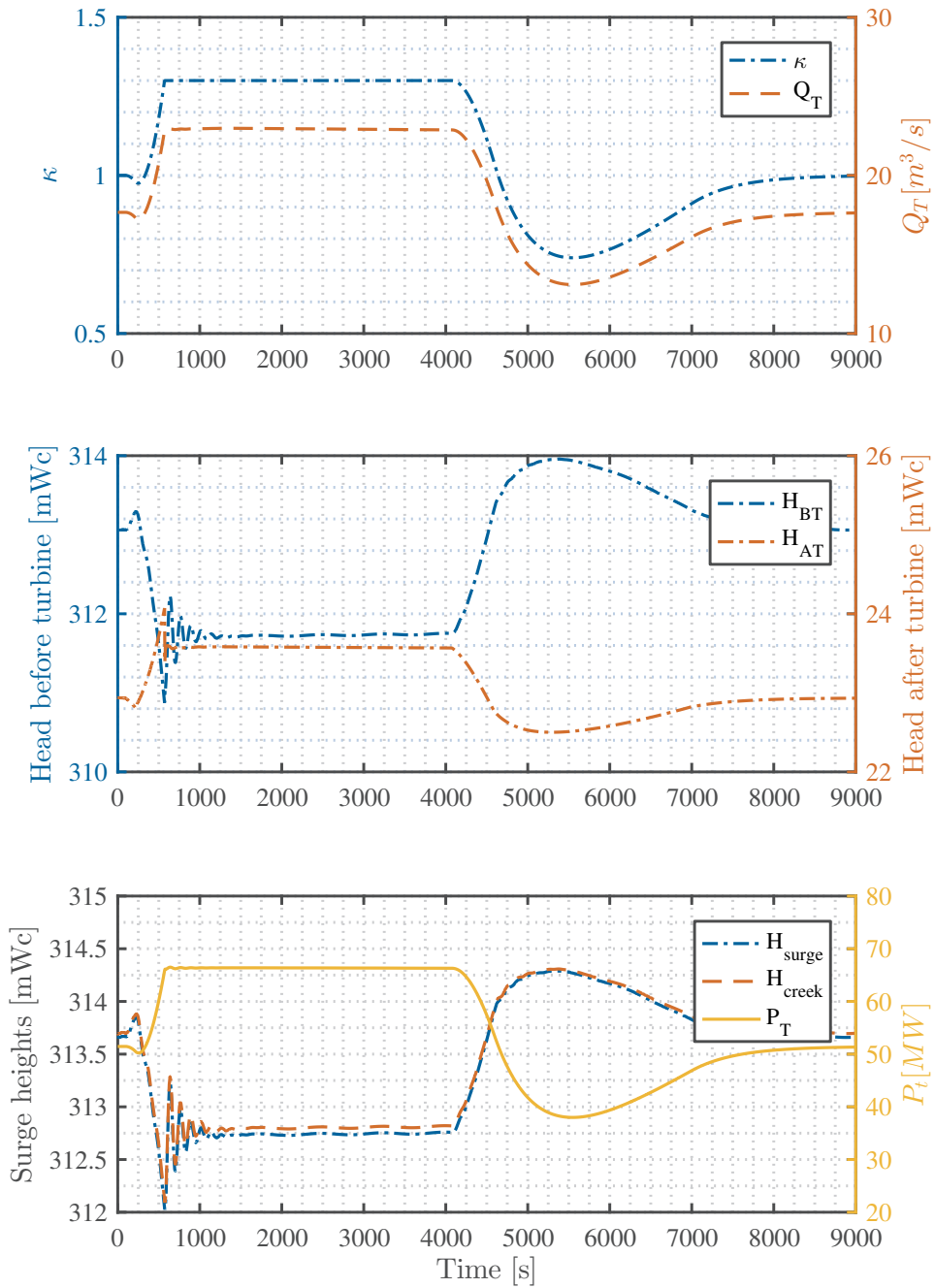
Figure 6.4: Conduit behavior for reference case
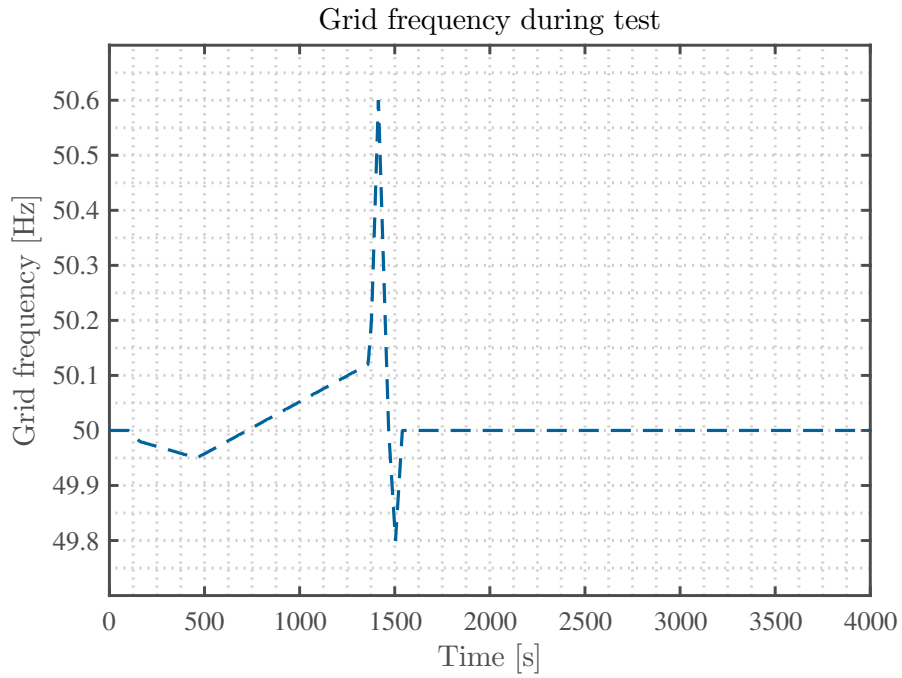
Figure 6.5: Input frequency with the loss of a large electrical load
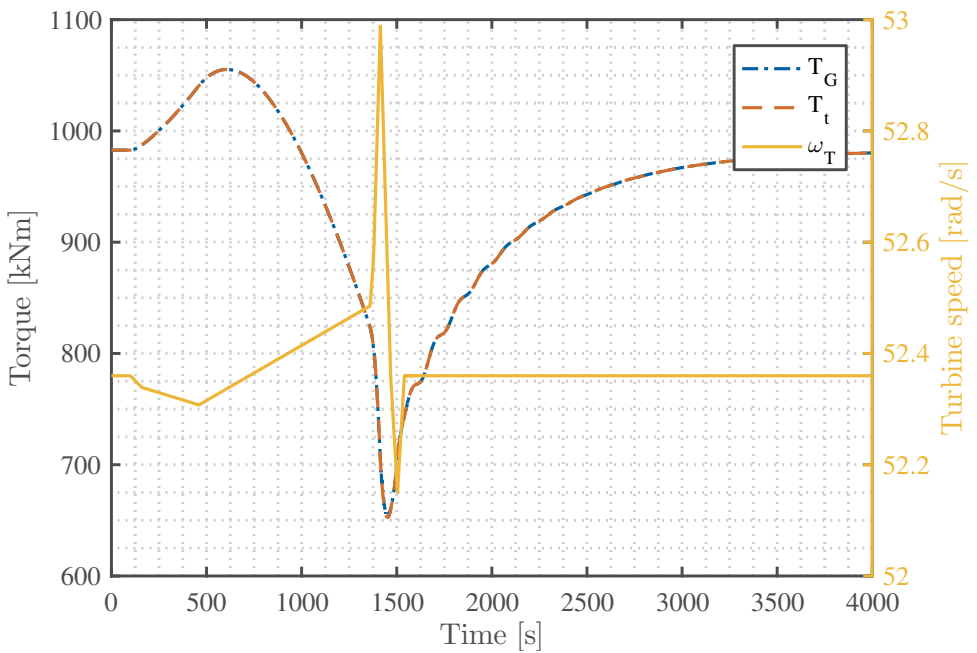
Figure 6.6: Speed and torque of turbine and generator when frequency as in figure 6.5
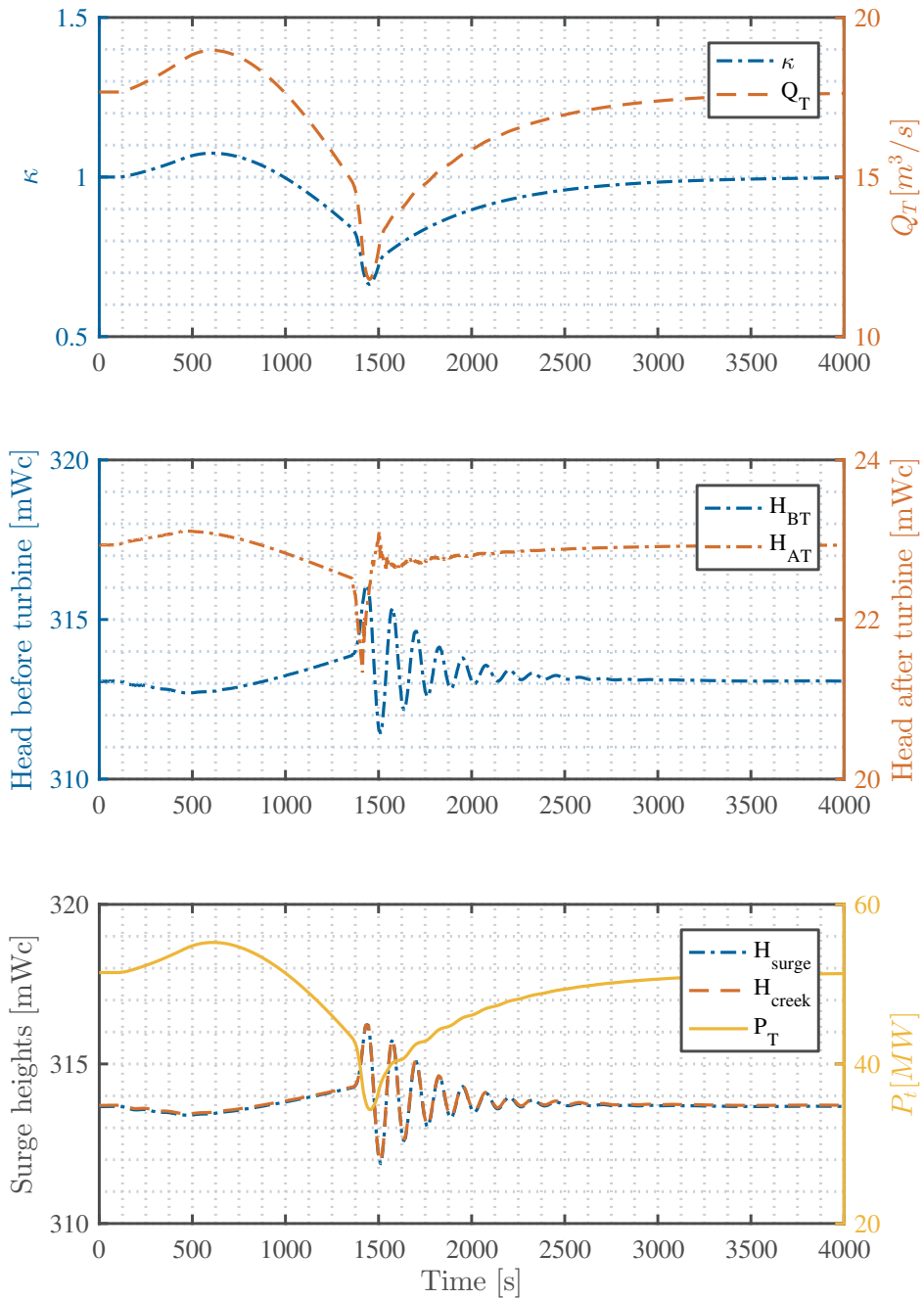
Figure 6.7: Conduit and turbine behavior when frequency behaves like in figure 6.5
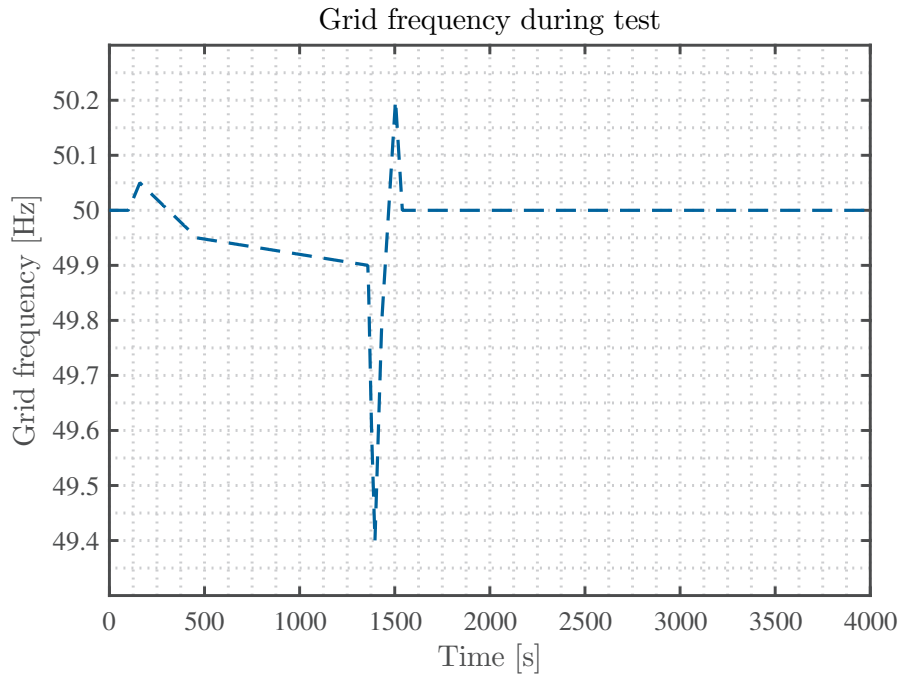
Figure 6.8: Input frequency simulating the sudden loss of a large production facility
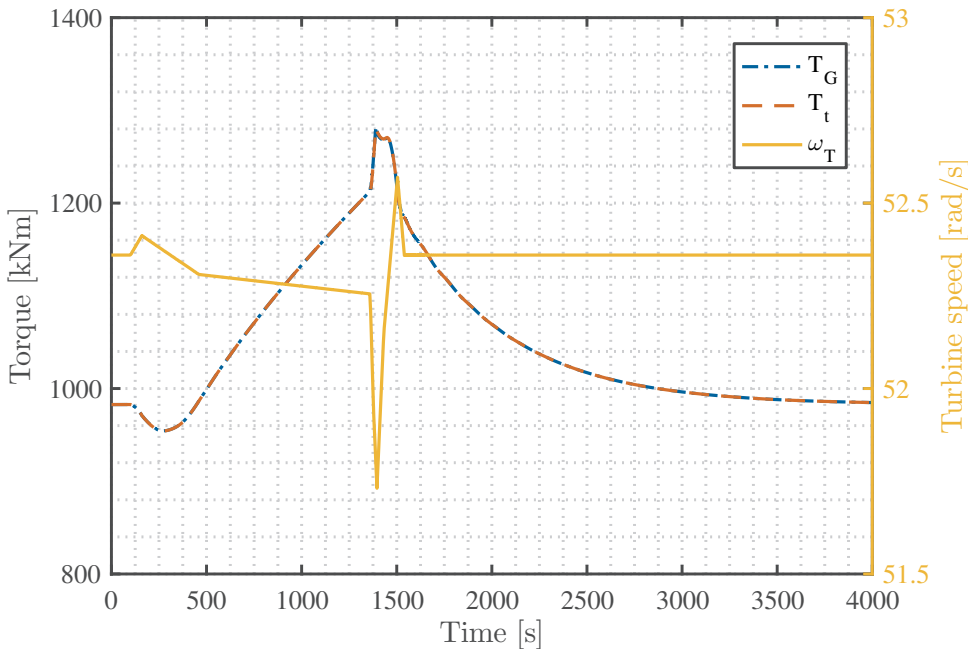
Figure 6.9: Speed and torque of turbine and generator when frequency as in figure 6.8
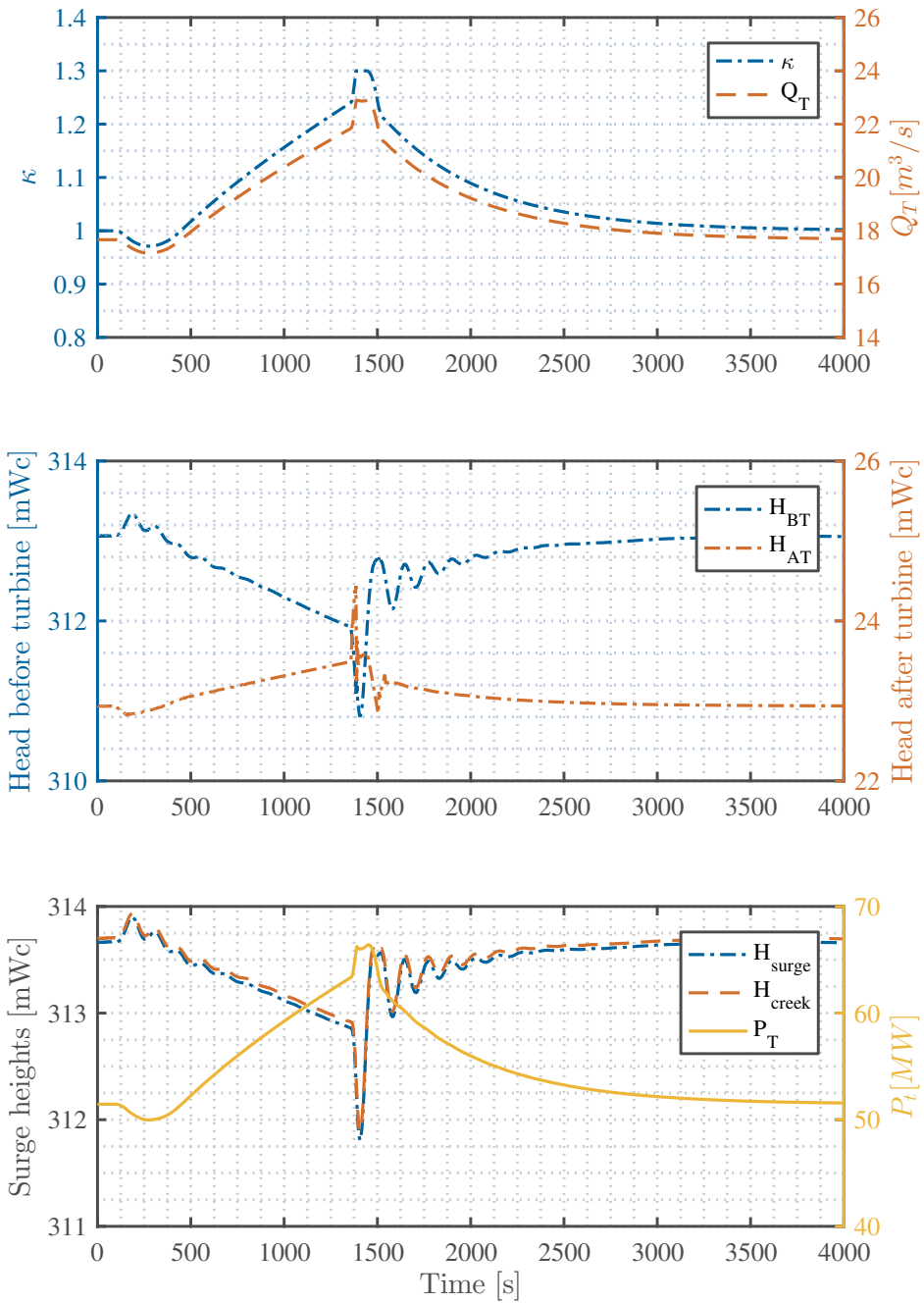
Figure 6.10: Conduit and turbine behavior when frequency behaves like in figure 6.8

7 | Discussion

7.1 Measurements on Bruvollelva

The two tests that were preformed at the power plant yielded quite ambiguous results. The first test (figure 5.3) gave no indication that the hydraulics in the power plant should influence the fault ride through properties of the generator. In fact there were no indications on the pressure measurements of a voltage drop.

During the second test the generator disconnected. Why this happened is unclear and the measurements is showing a pressure rise that reassembles a full load rejection. The measure pressure in front of the turbine almost doubles in a time span of about four seconds (figure 5.4). It is worth mentioning that this looks like a classical water hammer measurement. Due to the lack of measurements of the turbine speed it is hard to say exactly what caused the load rejection. Two possible scenarios immediately comes to mind:

- A safety mechanism of sorts is activated when the generator disconnects and the runner accelerates. This closes the guide vanes and the pressure rise comes of the rapid closure and following change in volume flow going through the runner.

- The turbine rotational speed increases due to the lack of generator torque. The self governing of the turbine leads to a full load rejection.

Which of the above that actually occurs is hard to decide upon with the pressure in front of the turbine being the only parameter that was measured.

7.2 Simulations of Bruvollelva power plant

Due to the lack of measured data in the water hammer measurements in Bruvollelva the simulations are done to try providing a more complete dataset. The first simulation was done by keeping the generator connected to the turbine while closing the guide vanes in a time span of four seconds. In figure 5.5 the pressure-time progress along with a couple of other simulated values. The amplitude seems to fit quite well with the measured results but the phase of the simulated values are shifted quite far away from the measurements after the first amplitude.

The second simulation of Bruvollelva shows the behavior of the power plant with the sudden loss of generator torque. As seen in figure 5.6 the turbine rotational speed doubles in about ten seconds

after the generator torque is set to zero. The self governing of the turbine increases the flow trough the turbine as the turbine speed increases. The change in pressure following the increasing volume flow can bee seen in the second sub-figure. The change in pressure is however lots smaller than in the previous simulation and does not fit with the measured result.

Since the two simulations above could not explain the water hammer measurements to a full extent the two simulation were combined. Since the measurements on the electrical part shows that the generator disconnects during the voltage drop this was needed as an input. To be able to explain the pressure rise the guide vanes are closed in four seconds. The results here shows a water hammer measurements that looks quite alike the measured values.

Of these three cases listed above the last one is the one that seems to fit best with the measured data and known input values. The pressure in both case one and three fit well considering the first pressure spike and dampening over time but the phase of the simulated values does not compare well with the measurements. This is however a classical problem with water hammer simulations. A more accurate result would most likely require a more advanced transient friction model. An example of how this could be implemented may be found in the doctoral thesis of Storli [20]. A more advanced transient friction model would however increase the simulation time, making the system of equations for the pipe sections semi-implicit and therefore more computationally demanding.

7.3   Simulations of Bogna power plant

As seen from chapter 6 the changing grid frequency will influence the surge arrangements and the pressure in front of the turbine and in the draft tube. The fluctuations are however rather small (the peak-to-peak values of the fluctuations are never larger than four meters) and they are quickly dampened out. It is highly unlikely that such fluctuations will damage the equipment in the hydro power plant. However if these spikes in frequency comes in rapid succession this might lead to pressure fluctuation that never really settle. There are however little evidence in the simulations that this might be a big problem. In general it may look like the frequency changes are to slow to provoke any large pressure waves of significance. The frequency governor with the speed droop does its best to compensate for the changing frequency and it seems to work quite well.

Such fluctuations may however influence the sand traps in the power plant. Pressure fluctuations such as the ones shown in chapter 6 might stir up sand that previously has been trapped in the sand traps. An increased amount of sand through the guide vanes and the runner will cause extra erosion wear on the mechanical parts in the power plant. Where the sand traps are located are however unknown and it is not sure if the sand traps will be influenced of the pressure fluctuations at all. From these simulations Bogna power plant look well equipped for handling a more varying frequency than what we have today.

8 | Conclusion

8.1 Bruvollelva power plant

The main task of this thesis was to find out if the hydraulic elements in a small hydro power plant would influence the generators ability to satisfy the Fault Ride Through properties. More measurements are needed to say something definite but the measurements done at this theses does not point to such a conclusion. The question is however if the generator is supposed to disconnect at all during the tests preformed, which were considered quite mild compared to what the power plant is supposed to handle without trouble. According to *FIKS* the generator should be able to handle this without any trouble. The water hammer which was measured during the second test is not supposed to happen in any way in such a small power plant. It is highly unlikely that the power plant is dimensioned for such pressure spikes and they will most certainly degrade the equipment severely over time.

One of the main task with this thesis was to investigate if and to what degree the dynamics in the conduit system and the turbine would influence the generators ability to fulfil the Fault Ride Through properties listed in *FIKS*. As the measured data shows the power plant does not fulfil the FRT requirements. There should also be taken action to ensure that such pressure increases as the one measured in case number two does not occur again.

8.2 Bogna power plant

The simulations of Bogna shows no signs of the power plant being unable to handle the simulated frequency deviations. As a matter of fact Bogna seems able to handle much sharper changes than what is considered here and to do so in style. There are however some uncertainties concerning where the sand traps in the power plant might be located and of it/they (there might be several sand traps) might be influenced by the variation in hydraulic pressure. This might lead to a larger sand load through the runner than usual that might in turn lead to more wear of the mechanical equipment. There are however no data to support this, only speculation.

9 | Further Work

The model seems to work satisfactory for most simulations that are done in this thesis. There are however a couple of improvements that would increase the accuracy of the simulation:

A more advanced friction model could be implemented. The model used in this thesis is very simple but seems to model the dampening of the water hammer transients satisfactory with some calibration of the transient friction factor, k_t. A calibration of this constant would however require physical measurements of the power plant, which is something that is not always easy to get hold of. The model does not manage to model the phase change during the large hydraulic transients satisfactory. A more advance model might handle this better but it is far from certain.

The turbine model needs a couple of improvements. It is not able to handle the closed state (κ = 0). Fixing this would be a major improvement of the model and make it able to handle most simulations of a hydro power plant. Another improvement of the turbine model would be to implement the pump turbine model.

The model for the generator and voltage governing showed difficult to implement in Simulink. The accuracy of the model are also questionable. An accurate model of the grid and generator are a must when modeling the FRT properties and behavior of the power plants. A more accurate model of both the grid and generator would likely improve the accuracy of the simulations. Another implementation of the connection between the generator and the voltage governor should also be considered. The voltage governor does not seem to work properly in this simulation.

It still remains unclear of the hydraulics of a small hydro power plant will and to what degree will influence the Fault Ride Through properties. More measured data is therefore needed before a arriving to the final conclusion of whether and to what degree the hydraulics elements influences the Fault Ride Through properties of the power plant. Future measurement should also include measuring the turbine rotational speed, this would be an important input to future simulations.

[**This page is intentionally left blank**]

References

[1] American Society of Civil Engineers, ed. *Hydroelectric pumped storage technology: international experience*. New York, N.Y: American Society of Civil Engineers, 1996. 1 p.

[2] B Brunone, UM Golia, and M Greco. "Some remarks on the momentum equation for fast transients". In: *Proc. Int. Conf. on Hydr. Transients With Water Column Separation*. 1991, pp. 201–209.

[3] D M Bucur et al. "Simultaneous transient operation of a high head hydro power plant and a storage pumping station in the same hydraulic scheme". In: *IOP Conference Series: Earth and Environmental Science* 22.4 (Dec. 8, 2014), p. 042015.

[4] Yunus A Çengel and John M Cimbala. *Fluid mechanics: fundamentals and applications*. Singapore: McGraw-Hill Higher Education, 2010.

[5] Stephen J. Chapman. *Electric machinery fundamentals*. 5. ed., internat. ed. New York, NY: McGraw-Hill, 2012. 680 pp.

[6] Mohamed S. Ghidaoui et al. "A Review of Water Hammer Theory and Practice". In: *Applied Mechanics Reviews* 58.1 (2005), p. 49.

[7] Even Lillefosse Haugen. "Master Thesis Even Lillefosse Haugen". Master thesis. Trondheim, Norway: NTNU, 2013. 117 pp.

[8] Hermod Brekke. *Pumper & Turbiner*. Vannkraftlaboratoriet, NTNU, 2003.

[9] Torbjorn K Nielsen. "Transient characteristics of high head Francis turbines". In: *Doctoral theses* (1990).

[10] Torbjørn K. Nielsen. "Simulation model for Francis and Reversible Pump Turbines". In: *IJFMS* 8.3 (2015), pp. 169–182.

[11] Torbjørn Kristian Nielsen. *Dynamisk Dimensjonering av Vannkraftverk*. SINTEF Strømningsmaskiner, Dec. 18, 1990, p. 117.

[12] Torbjørn Kristian Nielsen. "Simulation of The Dynamic Behaviour of Governing Turbines Sharing the same Electrical Grid". In: IAHR Workgroup. Slovenia, 1995, p. 10.

[13] Torbjørn Kristian Nielsen and Finn O. Rasmussen. "Analytic Model for Dynamic Simulations of Francis Turbines - Implemented in MOC". In: IAHR. San Paulo, 1992, p. 11.

[14] Alireza Riasi, Mehrdad Raisee, and Ahmad Nourbakhsh. "Simulation of transient flow in hydroelectric power plants using unsteady friction". In: *Strojniški vestnik-Journal of Mechanical Engineering* 56.6 (2010), pp. 377–384.

[15] SINTEF Energi. *DipLab - Mobilt kortslutningslaboratorium*. 2016. URL: `https://www.sintef.no/projectweb/diplab/` (visited on 05/30/2016).

[16] Jerko Škifić et al. "Numerical simulations of hydraulic transients in hydropower plant Jajce II". In: *Engineering Review* 33.1 (2013), pp. 51–56.

[17] Småkraft. *Bruvollelva kraftverk, Snåsa*. 2016. URL: `http://www.smaakraft.no/aktuelt/nyhetsarkiv/bruvollelva-kraftverk_-snasa/` (visited on 11/22/2015).

[18] Eivind Solvang et al. "Norwegian hydropower for large-scale electricity balancing needs". In: (2014).

[19] Statnett. *FIKS*. 2012.

[20] Pål-Tore Storli. "Transient friction in pressurized pipes; the water hammer phenomenon". 2010.

[21] Ronald E Walpole. *Probability & statistics for engineers & scientists*. Boston, Mass.: Pearson, 2012.

[22] E. Benjamin Wylie and Victor L. Streeter. *Fluid transients*. 3rd ed. 1983. 384 pp.

[23] Ming Zhao and Mohamed S Ghidaoui. "Godunov-type solutions for water hammer flows". In: *Journal of Hydraulic Engineering* (2004).

A | The method of characteristics used on Allievi's equations

A.1 Transformation of Allievi's equations

The method described in here is the one used in *Fluid transients* by Wylie and Streeter. This is a much used and well known method often used to simulate transients in different applications in fluid flow.

The fundamental equations in this method is the Allievi's equations that describes the momentum and the continuity equation for one dimensional fluid flow. These are valid for slightly compressible flow. The equations are shown below:

$$L_1 = \frac{\partial H}{\partial x} + \frac{1}{gA}\frac{\partial Q}{\partial t} + h_f = 0 \tag{A.1.1}$$

$$L_2 = \frac{\partial H}{\partial t} + \frac{a^2}{gA}\frac{\partial Q}{\partial x} = 0 \tag{A.1.2}$$

By multiplying equation (A.1.2) with an unknown multiplier, λ, and adding it to equation (A.1.1) the following expression arises:

$$\frac{\partial H}{\partial x} + \frac{1}{gA}\frac{\partial Q}{\partial t} + h_f + \lambda\left(\frac{\partial H}{\partial t} + \frac{a^2}{gA}\frac{\partial Q}{\partial x}\right) = 0 \tag{A.1.3}$$

By organising the above equation after the main parameters, Q and H, the above equation will look like:

$$\lambda\left(\frac{\partial H}{\partial t} + \frac{1}{\lambda}\frac{\partial H}{\partial x}\right) + h_f + \frac{1}{gA}\left(\frac{\partial Q}{\partial t} + a^2\lambda\frac{\partial Q}{\partial x}\right) = 0. \tag{A.1.4}$$

The chain rule for dH/dt and dQ/dt yields

$$\frac{dH}{dt} = \frac{\partial H}{\partial t} + \frac{dx}{dt}\frac{\partial H}{\partial x}, \tag{A.1.5}$$

$$\frac{dQ}{dt} = \frac{\partial Q}{\partial t} + \frac{dx}{dt}\frac{\partial Q}{\partial x}. \tag{A.1.6}$$

By comparing (A.1.4) to (A.1.5) and (A.1.6) and solving for dx/dt to find the characteristic lines for the system of equations:

$$\frac{dx}{dt} = \frac{1}{\lambda} = a^2\lambda \tag{A.1.7}$$

This corresponds to the characteristic lines for the Allievi's equations. These may be expressed as a function of the unknown multiplier, λ:

$$\frac{dx}{dt} = \frac{1}{\lambda} = \pm a \qquad\qquad\qquad \text{(A.1.8)}$$

The two characteristic lines are inserted into (A.1.4) and the following system of ordinary differential equations arises:

$$\frac{1}{a}\frac{dH}{dt} + \frac{1}{gA}\frac{dQ}{dt} + h_f = 0, \qquad \frac{dx}{dt} = a \qquad\qquad \text{(3.1.3a)}$$

$$-\frac{1}{a}\frac{dH}{dt} + \frac{1}{gA}\frac{dQ}{dt} + h_f = 0, \qquad \frac{dx}{dt} = -a. \qquad\qquad \text{(3.1.3b)}$$

This system is integrated and the algebraic system of equations that arises here may be used to simulate dynamic behavior of a fluid system.

B | The turbine model

The turbine model used to simulate the behavior of the turbine in this thesis is taken from the PhD thesis by Nielsen [9]. Some input is (especially for the dimensionless part) is taken from the article "Simulation model for Francis and Reversible Pump Turbines" by the same author [10].

B.1 Normal form

The change in momentum going through the turbine may be described by the differential equation below:

$$I\frac{dQ}{dt} = \rho g H_e - \rho g H_R \left(\frac{Q}{\kappa Q_R}\right) - \rho s \left(\omega_t^2 - \frac{H_e}{H_R}\omega_{t_R}^2\right). \tag{B.1.1}$$

Here s is the self regulating parameter of the turbine and I is the hydraulic inertia of the turbine. The hydraulic inertia of the turbine represents the mass and inertia of the water inside the runner as well as the amount of water in the spiral casing and the draft tube. The self regulating parameter is a constant that is defined by the geometry of the runner and may be calculated from equation (B.1.2):

$$s = \frac{1}{8}D_1^2 \left(1 - \frac{D_2^2}{D_1^2}\right). \tag{B.1.2}$$

This parameter defines the behavior of the turbine when moving away from BEP. The change in turbine speed may also be described by a similar differential equation as the momentum:

$$J\frac{d\omega_t}{dt} = T_t - T_g \tag{B.1.3}$$

$$T_t = \rho Q(r_1 c_{u_1} - r_2 c_{u_2}). \tag{B.1.4}$$

This form requires a lot of computational steps to find the c_u-components. A more user friendly version is show in equation (B.1.5):

$$T_t = \rho Q \left(t_s - \frac{D_2^2}{4}\omega_t\right) \cdot \eta_h - R_m \left(\frac{\omega_t}{\omega_{t_R}}\right)^2. \tag{B.1.5}$$

Here t_s is the specific starting torque for the turbine, denoted as the torque per kilos of water per second ($N/_{kg\,s}$). This is computed by the dimensionless starting torque, m_s, and the rated specific

torque, t_R: $t_s = m_s t_R$. The specific rated torque may be computed by: $t_R = {gH_R}/{\omega_R}$

$$m_s = \xi \frac{q}{\kappa}(\cos\alpha_1 + \tan\alpha_{1_R}\sin\alpha_1) \tag{B.1.6}$$

Here the reduced flow, q, is used for the computation. The machine constant ξ is also used in equation (B.1.6). This is a machine constant described at BEP. Another machine constant that is used in the dimensional turbine model is the pressure number, ψ. These two constant may be computed using:

$$\psi = \frac{u_{2_R}^2}{gH_R} \tag{B.1.7} \qquad\qquad \xi = \frac{u_{1_R}c_{1_R}}{gH_R} \tag{B.1.8}$$

To model the turbine behavior properly, especially outside the BEP the efficiency of the turbine needs to be considered. This may be computed as a sum of the viscous losses and the losses that rises due to mismatched angles at in- and outflow. How these losses may be computed will bee thoroughly investigated in the next section.

B.2 Dimensionless form

All the equations described in section B.1 can be made dimensionless by using the the values of the turbine at BEP. Equation (B.1.1) and (B.1.3) may be written on dimensionless form as:

$$T_{wt}\frac{dq}{dt} = h - \left(\frac{q}{\kappa}\right)^2 - \sigma(\tilde\omega^2 - 1) \tag{B.2.1}$$

$$T_a\frac{d\tilde\omega}{dt} = \underbrace{\frac{q}{h}(m_s - \psi\tilde\omega)\eta_h - R_m\tilde\omega_t^2}_{T_t/T_{t_R}} - \underbrace{\eta_G}_{T_G/T_{t_R}} \tag{B.2.2}$$

where the new terms dimensionless are as following:

$$q = \frac{Q}{Q_R} \tag{B.2.3} \qquad\qquad h = \frac{H}{H_R} \tag{B.2.4}$$

$$\tilde\omega = \frac{\omega}{\omega_R} \tag{B.2.5} \qquad\qquad \sigma = s\frac{\omega_R^2}{gH_R} \tag{B.2.6}$$

The efficiency of the turbine is defined as

$$\eta_h = 1 - \frac{\Delta h}{h} \tag{B.2.7}$$

where Δh may be found as a sum of the viscous losses in the runner and the losses that arise when running the turbine away from BEP.

$$\Delta h = R_f q^2 + (R_d + R_c)(q - q_c)^2 \tag{B.2.8}$$

Here q_c is the flow that flows past the runner without doing any work, R_f is the loss constants that represent the viscous losses in the runner. R_c and R_d is the loss constants representing the losses at the inlet and the draft tube losses. These will only matter when the runner is operating away from BEP. These can not be calculated analytically and needs to be found by trial and error. q_c is a function of the speed of the runner and the guide vane angles and may be calculated by:

$$q_c = \tilde{\omega}_t \left(\frac{1 + \frac{\tan \beta_{1_R}}{\tan \alpha_{1_R}}}{1 + \frac{\tan \beta_{1_R}}{\tan \alpha_1}} \right) \tag{B.2.9}$$

By using the definition of the hydraulic efficiency of the runner and demanding that the derivative of the efficiency is zero at BEP the following connection between the pressure number (B.1.7) and inlet spin (B.1.8) arises:

$$\xi = (\eta_{h_R} + \psi) \cos \alpha_{1_R}. \tag{B.2.10}$$

The dimensionless self regulating parameter may also be expressed as a function of the pressure number and the rated hydraulic efficiency:

$$\sigma = \frac{\eta_{h_R} - \psi}{\eta_{h_R} + \psi}. \tag{B.2.11}$$

The rated hydraulic efficiency, η_{h_R}, is set to 0.96 for design purposes and for simulation purposes this works as a good assumption. The hydraulic efficiency may be modified by choosing the loss coefficients described in section B.3. This model is based on the Euler turbine equations. For some prototypes the deviations from these design conditions due to the corrections for synchronous speed and other demands such as demand for inlet/outlet blade angles making it possible to weld the runner the inlet spin and dimensionless self governing parameter calculated with equations (B.2.10) and (B.2.11) may not correspond with equations (B.1.8) and (B.2.6). To be able to model and simulate a reasonable turbine behavior along the whole operating area ξ and σ is calculated using equations (B.2.10) and (B.2.11).

B.3 The turbine on MOC form

To make the model compatible with the pipe model equations (B.2.3) and (B.2.1) has to be rewritten in terms of the previously explained terms. Here n denotes values from the previous time step. The terms that arises are now:

$$q(m_s - \psi\tilde{\omega})\eta_h - R_m\tilde{\omega}_t^2 - \frac{T_G}{T_{t_R}} - \frac{T_a}{\Delta t}(\omega - \omega^n) = 0 \tag{B.3.1}$$

$$HC - B_t Q_R q - H_S - H_R \frac{1}{1+\sigma}\left[\left(\frac{q}{\kappa}\right)^2 + \sigma\tilde{\omega}^2 + R_{q\kappa}(q - q_c)\right]$$
$$- H_R \frac{T_a}{\Delta t}(q - q^n) = 0 \tag{B.3.2}$$

where the unknowns may be found using values for pressure and flow in the left node just before the turbine and the right node just after the turbine:

$$HC = C_{P_L} - C_{M_R} \tag{B.3.3}$$
$$C_{P_L} = H_L + B_L Q_L - R_L Q_L |Q_L| \tag{B.3.4}$$
$$C_{M_R} = H_R - B_R Q_R + R_R Q_R |Q_R| \tag{B.3.5}$$
$$B_t = B_L + B_R \tag{B.3.6}$$

The terms described above is the governed turbine taken from *Fluid transients*, rewritten to fit the turbine model by Nielsen. All other terms are as before, it is just the differential equations that need rewriting. These equation together with the governing equations may now be solved using a Newton solver.

C | Layout of Bogna Power Plant

Table C.1: Table with marked dimensions on Bogna sketch

Section	Length L [m]	Area A [m^2]	Propagation speed, a [m/s]	Roughness ϵ [m]
Head race	3345	15	1200	1e-2
Section 1	95	15	1200	1e-2
Section 2	120	13	1200	1e-2
Penstock	350	13	1200	1e-2
Section 3	45	$\in[13\ 50]$	1200	1e-2
Turbine pipe	60	5	1400	1e-4
Draft tube	24	7.5	1400	1e-4
Tail race	2356	15	1200	1e-2

Bangsjø

$HRV = 315\,MOH$

$LRV = 305\,MOH$

A_1, L_1

A_2, L_2

A_P, L_P

A_{HR}, L_{HR}
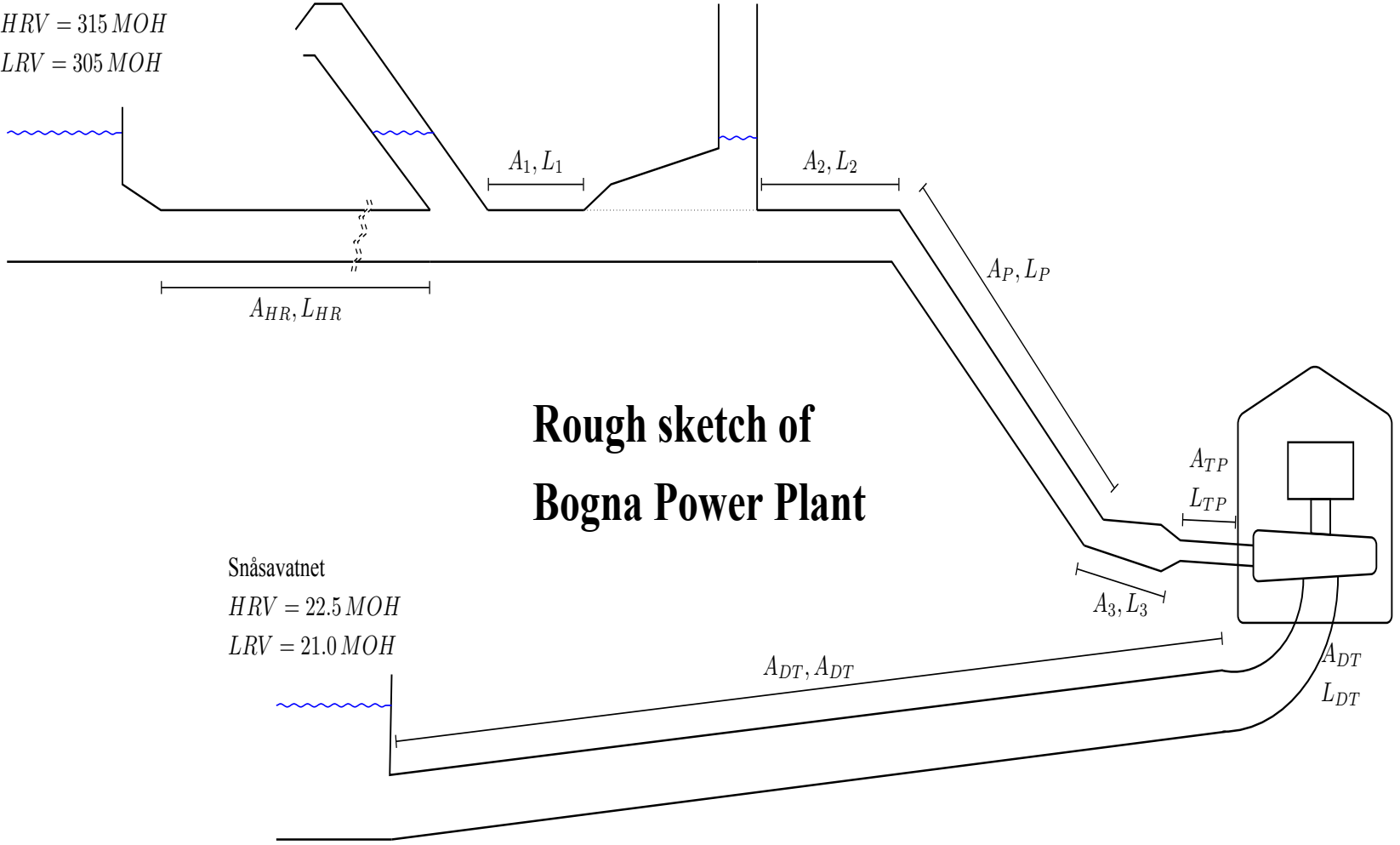
Rough sketch of

Bogna Power Plant

A_{TP}

L_{TP}

Snåsavatnet

$HRV = 22.5\,MOH$

$LRV = 21.0\,MOH$

A_3, L_3

A_{DT}, A_{DT}

A_{DT}

L_{DT}

D | Unfiltered measurements of Bruvollelva

First FRT test

First FRT test, smoothed data
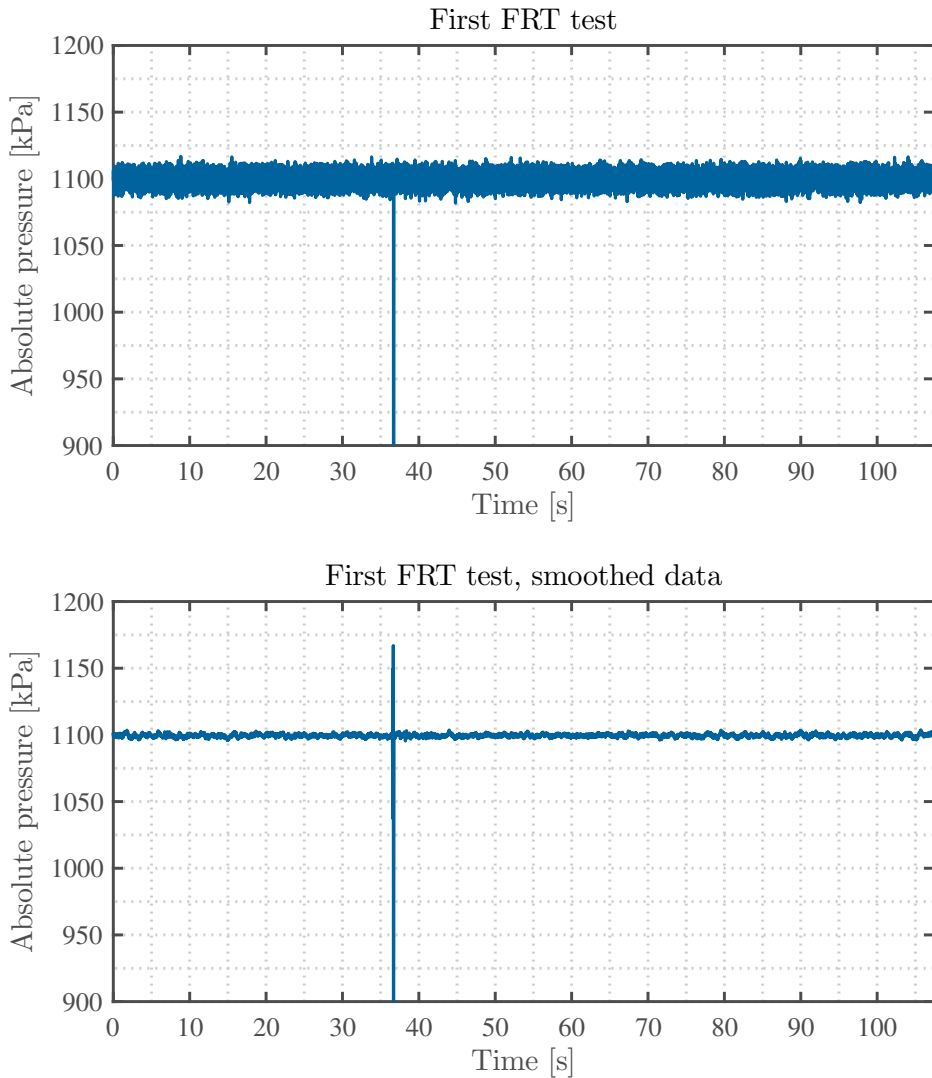
Figure D.1: Unfiltered and filtered data from the first test done at Bruvollelva
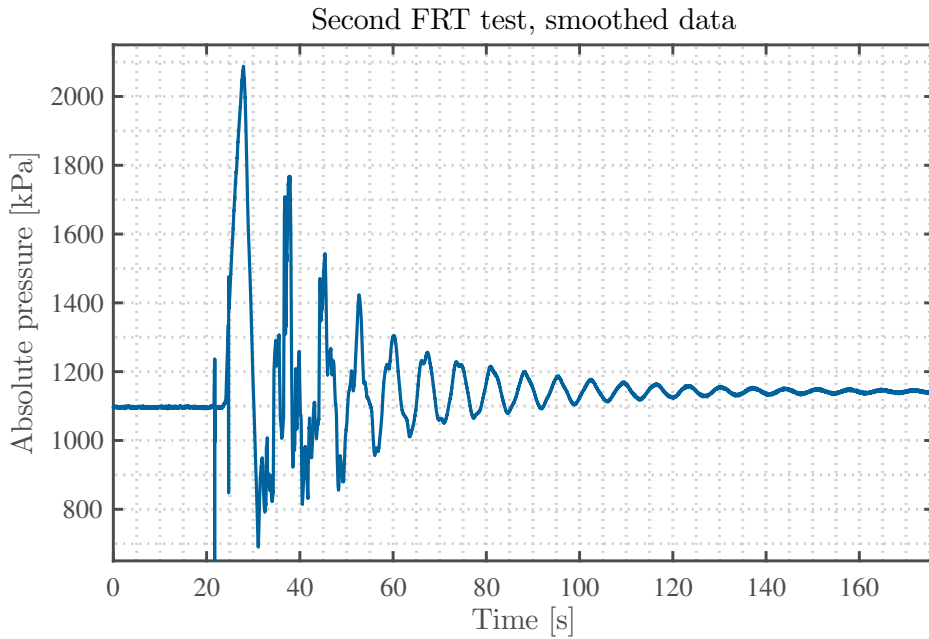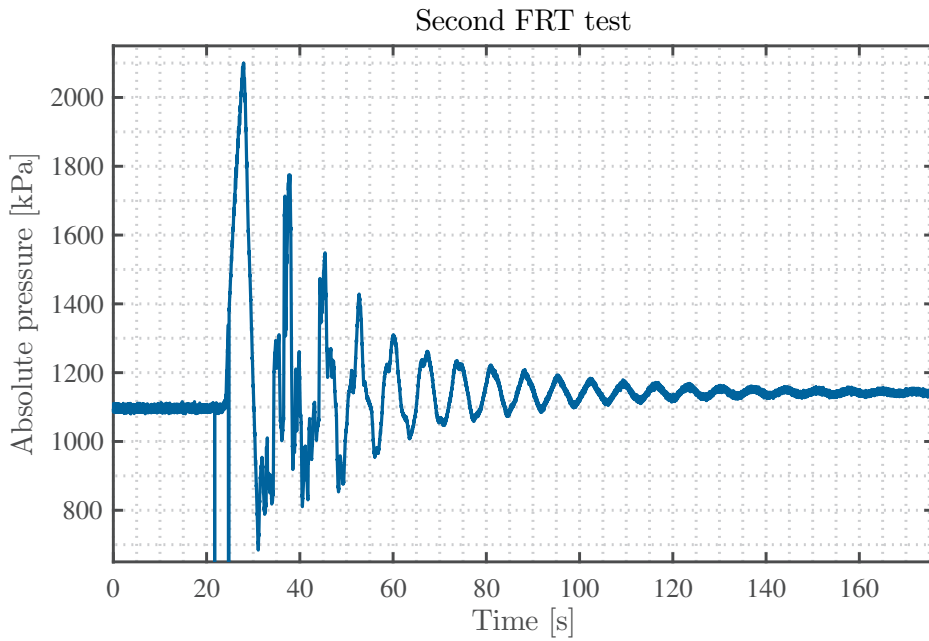
Figure D.2: Unfiltered and filtered data from the second test done at Bruvollelva

E | SINTEF measurements at Bruvollelva

E.1 First FRT test
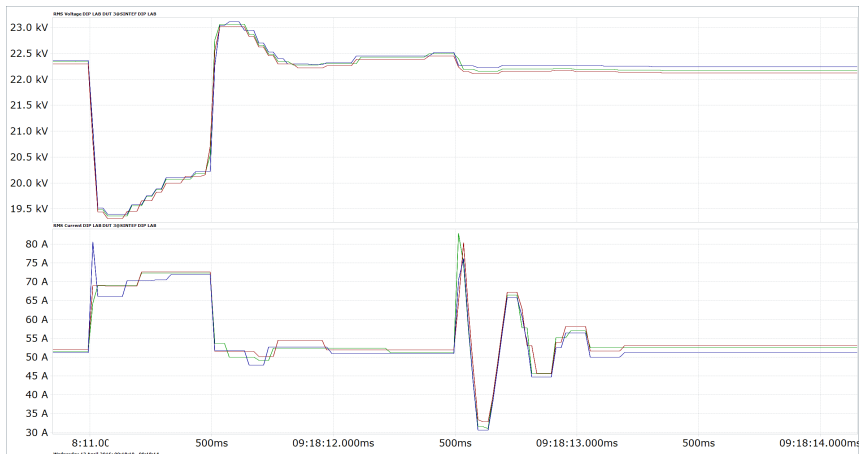
Figure E.1: Data logged in the DIP-lab of the first FRT test

E.2 Second FRT test
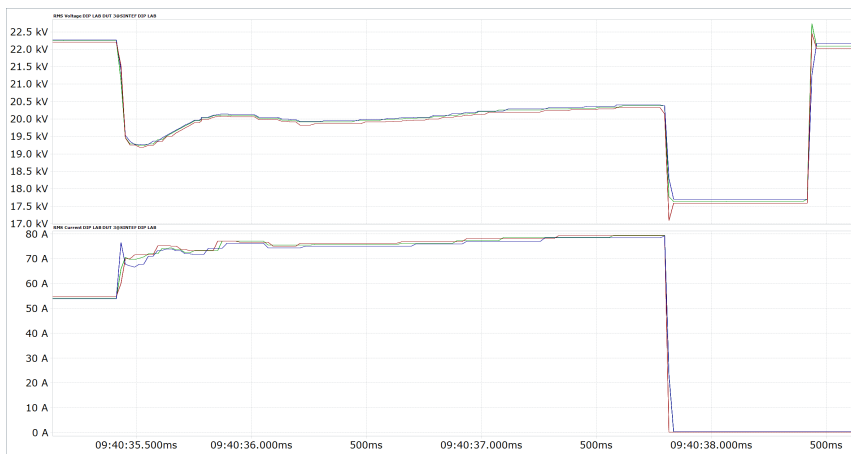
Figure E.2: Data logged in the DIP-lab of the second FRT test

F | Initialization code for power plants

Bruvollelva

```matlab
%%%%%%%%%%%%%%%%%%%%%%%%%%%%%%%%%%%%%%%%%%%%%%%%%%%%%%%%%%%%%%%%%%%%%%%%%%%
%%%% Values for the power plant Bruvollelva        %%%%%%%%%%%%%%%%%%%%%
%%%%                                               %%%%%%%%%%%%%%%%%%%%%
%%%%                                               %%%%%%%%%%%%%%%%%%%%%
%%%%%%%%%%%%%%%%%%%%%%%%%%%%%%%%%%%%%%%%%%%%%%%%%%%%%%%%%%%%%%%%%%%%%%%%%%%
clc
clear all

% Fundamental constants %%%%%%%%%%%%%%%%%%%%%%%%%%%%%%%%%%%%%
g       = 9.81;            % gravitational constant
rho     = 1000;            % densety of water
nu_water= 1e-6;            % Dynamic viscosiy of water at 10 C
%%%%%%%%%%%%%%%%%%%%%%%%%%%%%%%%%%%%%%%%%%%%%%%%%%%%%%%%%%%%%

% Data for the pipes
D_pipe  = 1.2;
D_grp   = D_pipe;
D_iron  = D_pipe;
A_pipe  = pi*D_pipe^2/4;% random area of conduit
L_grp   = 1100;            % length of GRP pipe
L_iron  = 250;             % length of iron pipe
total_length = L_grp+L_iron;
%%%%%%%%%%%%%%%%%%%%%%%%%%%%%%%%%%%%%%%%%%%%%%%%%%%%%%%%%%%%%%%%%%%%%%%%%%%
% a       = 1200;          % approximate speed of sound for a conduit filled with ...
    water
a_iron  = 1415;            % speed of sound in a cast iron pipe
a_grp   = 894;             % speed of sound in a GRP pipe
% Above values computed from formula in "Dynamisk dimensjonering av
% vannkraftverk", p. 26, assuming a pipe thickness of 0.15 m

a_grp   = 800;             % assumed values for simplifying computations
a_iron  = 1400;            % "real" values above

n_grp   = 154;
n_iron  = 20;
dx_grp  = L_grp/n_grp;
dx_iron = L_iron/n_iron;

dt_ = dx_iron/a_iron;
```

```matlab
H_res = 117; H_lres = 0;

totL_grp    = n_grp*dx_grp;
totL_iron   = n_iron*dx_iron;

fprintf('Chosen time step: %.6f \n', dt_)
fprintf('This gives a total pipe length of %.2f m\n\n' , totL_grp + totL_iron)
fprintf('with GRP pipe length of %.2f m \n', totL_grp)
fprintf('and IRON pipe lenght of %.2f m \n', totL_iron)

%%%% Calculate correct values for a for different types of pipes
H0      = 117;              % total head (without losses)
Q0      = 3.85;            % max flow through the turbine

% Design values for the hydro turbine
n_R     = 750;             % Rated rotational speed of the turbine
omega_R = n_R*pi/30;
H_R     = 110;             % Rated head [m] from data sheet
Q_R     = 0.9*Q0;          % Rated flow [m^3/s] from data sheet
eta_t   = 0.919;           % Hydraulic efficiency
Pmax = 3.9e6;
% eta   = [ 0.73   81.5   88.5   91.0   91.8   91.9   91.7]; Real eta from chart
% Q/Q_max=[ 0.4    0.5    0.6    0.7    0.8    0.9       1];

% Geometrical parameters of the turbine
D1      = 0.84;         % calculated from information given
D2      = 0.9;          % given from data sheet
B1      = 0.241;            % calculated from information given
Ta      = 2;
Twt     = 0.1;
% Twt = input('Tubine inertia time constant goes here: '); fprintf('\n')


% Calculating different velocity components in the turbine
% All values are for best point (cu2 = 0)
fprintf('D1 = %.2f \n', D1)
fprintf('Ta = %.2f \n', Ta)
fprintf('Twt = %.2f \n', Twt)

denom = sqrt(2*g*H_R);
u1 = omega_R*D1/2; u1_ = u1/denom; % assuming u1_ = 0.72
cm2 = Q_R*4/(pi*D2^2);
cm1 = Q_R/(pi*D1*B1);
cu1_ = 0.96/(2*u1_); cu1 = cu1_*denom; % hydraulic efficiiency, eta = 0.96 at BP
c1 = sqrt(cu1^2 + cm1^2);
u2 = omega_R*D2/2;
alfa1 = atan(cm1/cu1);
beta1 = atan(cm1/(u1-cu1));
beta2 = atan(cm2/u2);

xi = (u1*c1)/(g*H_R);
phi = (omega_R*D2/2)^2/(g*H_R);
```

```
% Generator values
delta_R = pi/4;

% Turbine regulator values

% Values obtained from Moody diagram in Cengel-Cimbala
epsilon_grp = 0;        % Absolute roughness for GRP pipe
epsilon_iron = 0.24e-3; % Absolute roughness for cast iron pipe
k_trans = 0.25;

% Friction fractors calculated with Colebrook formula
f_iron = 0.01;
f_grp = 0.0095;
% Grid and generator values
R_grid = 10;          % ohm
power_factor = 0.9;
T_gR = 55195;         % Nm
m_d = 0.01;           % dampening coefficient for generator

% setting initial conditions
Q0_t = 2.2;
H0_grp1 = H_res - f_grp*150*((Q0_t^2/(2*g*A_pipe*A_pipe*D_pipe)));
H0_i  = H0_grp1- f_iron*L_iron/2*(Q0_t^2/(2*g*A_pipe*A_pipe*D_pipe));
H0_grp2 = H0_i - f_grp*400*(Q0_t^2/(2*g*A_pipe*A_pipe*D_pipe));
H0_t = H0_grp2 - f_grp*400*(Q0_t^2/(2*g*A_pipe*A_pipe*D_pipe));

P0_t = rho*g*Q0_t*H0_t; omega0_t = n_R*pi/30;
T0_t = P0_t/omega0_t;
Q0_i = Q0_t; Q0_grp = Q0_t;
```

Bogna

```
% Values for Bogna power plant

clc
clear all
close all

% Physical constants %%%%%%%%%%%%%%%%%%%%%%%%%%%%%%%%%%%%%%%%%%%%%%%%%%%%%%%%%
g = 9.81;
rho_water = 1000;
nu_water = 1e-6;
epsilon_rock = 1e-2; epsilon_steel = 1e-4; k_trans = 0.25;

%% Turbine values and details %%%%%%%%%%%%%%%%%%%%%%%%%%%%%%%%%%%%%%%%%%%%%%%%

% Rated values
H_R_turbine = 270;                        % m
```

```matlab
Q_max_turbine = 24*2;                          % m^3/s
Q_R_turbine = 16.9*2;                          % m^3/s
P_R_turbine = 56e6*1.9;                        % W
n_r_turbine = 500;                             % rpm
omega_R = n_r_turbine*pi/30;                   % 1/s
Ta = 6;                                        % s
Twt = 0.2;                                     % s
T_R = P_R_turbine/omega_R;                     % rated torque


% Geometry values %%%%%%%%%%%%%%%%%%%%%%%%%%%%%%%%%%%%%%%%%%%%%%%%%%%%%%%%%
D1 = 2*1.5;                                    % m
D2 = 1.5*1.5;                                  % m
B1 = 0.33*1.5;                                 % m
%%%%%%%%%%%%%%%%%%%%%%%%%%%%%%%%%%%%%%%%%%%%%%%%%%%%%%%%%%%%%%%%%%%%%%%%%%%%


% Calculated rated turbine values %%%%%%%%%%%%%%%%%%%%%%%%%%%%%%%%%%%%%%%%%%
cm1 = Q_R_turbine/(D1*B1*pi);
cm2 = Q_R_turbine/(pi*D2^2/4);
u1 = omega_R*D1/2;
u2 = omega_R*D2/2;
u1_ = u1/sqrt(2*g*H_R_turbine);
eta_h = 0.96;
cu1_ = eta_h/(2*u1_);
cu1 = cu1_*sqrt(2*g*H_R_turbine);
c1 = sqrt(cu1^2+cm1^2);
%%%%%%%%%%%%%%%%%%%%%%%%%%%%%%%%%%%%%%%%%%%%%%%%%%%%%%%%%%%%%%%%%%%%%%%%%%%%
beta1 = atan(cm1/(u1-cu1));
beta2 = atan(cm2/u2);
alfa1 = atan(cm1/cu1);
%%%%%%%%%%%%%%%%%%%%%%%%%%%%%%%%%%%%%%%%%%%%%%%%%%%%%%%%%%%%%%%%%%%%%%%%%%%%
pressure_number = (u2^2)/(g*H_R_turbine); inlet_spin = (u1*c1)/(g*H_R_turbine);
fprintf([num2str(char(945)),'1 \t\t', num2str(char(946)),'1 \t\t', ...
    num2str(char(946)),'2 \n'])
fprintf('%.2f \t %.2f \t %.2f \n', alfa1*180/pi, beta1*180/pi, beta2*180/pi)


% Generator values %%%%%%%%%%%%%%%%%%%%%%%%%%%%%%%%%%%%%%%%%%%%%%%%%%%%%%%%%
T_gR =T_R*1.3;
delta_R = pi/4;
P = 3000*2/n_r_turbine;
R_grid = 10;
m_d =  0.05;
T_dg = 1.0;
delta_tg = 0.04;
delta_bg = 0.02;
T_G0 = T_R;
kphi0 = 80;
%% Tunnel data %%%%%%%%%%%%%%%%%%%%%%%%%%%%%%%%%%%%%%%%%%%%%%%%%%%%%%%%%%%%%
dt_calc;

% Reservoir
H_res = 315;
A_res = 15;
```

```matlab
D_res = sqrt(4*A_res/pi);
delta_x_res = dx_vec(1);

% Head race tunnel
L_in = 3440;                          % m
A_in = 15;                            % m^2
D_in = sqrt(4*A_in/pi);              % m
pressure_speed_in = 1200;            % m/s
delta_x_in = dx_vec(1);

% Surge shaft
shaft_elevation = 295;

% Tunnel between surge shaft & penstock
L_bet = 120;                          % m
D_bet = 4.05;                         % m
A_bet = pi*D_bet^2/4;                 % m^2
pressure_speed_bet = 1200;           % m/s
delta_x_penstock = dx_vec(3);

% Penstock
L_p = 350;                            % m
D_p = 4.05;                           % m
A_p = pi*D_p^2/4;                     % m^2
pressure_speed_P = 1200;             % m/s

% Shaft between penstock & turbine pipe
n_penSec = 5;                              % number of pipe sections
a_penSec = 1200;
D1_penSec = 4.05; A1_penSec =pi*D1_penSec^2/4;
A2_penSec = pi*2.25^2 + 4.5*2.45; D2_penSec = 4*A2_penSec/(4.50 + 2*2.45 + ...
    pi^2*2.25);
theta3 = 2*asin(6.3/(2*5.6));
A3_penSec = 6.3*7 + (5.6^2)/2*(theta3-sin(theta3)); D3_penSec = ...
    4*A3_penSec/(6.3+2*7+theta3*5.6);
delta_x_penSec = dx_vec(4);

% Turbine pipe
D_TP = 2.1;                           % m
A_TP = pi*D_TP^2/4;                   % m^2
L_TP = 53;                            % m
a_TP = 1400;                          % m/s
delta_x_TP = dx_vec(5);

% Draft tube
A_DT = 7.5;                           % m^2
D_DT = sqrt(4*A_DT/pi);              % m
a_DT = 1400;                          % m/s
delta_x_DT = dx_vec(6);              % m

% Tailrace
L_out = 2356;                         % m
```

```matlab
A_out = 15;                              % m^2
D_out = sqrt(4*A_out/pi);                % m
a_out = 1200;                            % m/s
delta_x_tailRace = dx_vec(7);            % m
H_lowerRes = 22;                         % m


%% Initial conditions %%%%%%%%%%%%%%%%%%%%%%%%%%%%%%%%%%%%%%%%%%%%%%%%%%%%%
% Turbine
% % H_res = H_res-H_lowerRes;
% H_lowerRes=0;
Q0_t = Q_R_turbine*1; omega0_t = omega_R; H0_t = H_R_turbine;

% Creek
H0_creek = 15;

% Head race tunnel
Q0_in = Q0_t; H0_in = H_res - 0.1*(L_in/2/D_in*Q0_in^2/(2*g*A_in^2));

% Surge shaft
H0_surge_shaft = H0_in - 0.1*(L_in/2/D_in*Q0_in^2/(2*g*A_in^2))-shaft_elevation;

% Penstock
Q0_penstock = Q0_t; H0_penstock = ...
    (H0_surge_shaft+shaft_elevation)-0.1*(L_p/2/D_p*Q0_penstock^2/(2*g*A_p^2));

% Shaft between penstock and turbine pipe
Q0_penSec = Q0_t; H0_penSec = ...
    (H0_surge_shaft+shaft_elevation)-0.1*(L_p/D_p*Q0_penstock^2/(2*g*A_p^2));

% Turbine pipe
Q0_TP = Q0_t; H0_TP = H0_penSec;

% Tail race
Q0_out = Q0_t; H0_out = H_lowerRes + 0.1*(L_out/2/D_out*Q0_out^2/(2*g*A_out^2));

% Draft tube
Q0_DT = Q0_t; H0_DT = H_lowerRes + 0.1*(L_out/D_out*Q0_out^2/(2*g*A_out^2));

% file names and path for saving in graphics folder of report
% load(fallingFileName.mat,risingFileName.mat,reference.mat);
% load(path.mat);
dt_=dt;
```

G | Uncertainty of measurements

G.1 Uncertainty analysis

A list of variables in use for the uncertainty analysis of the pressure measurements:

f_{ab} - Uncertainty of the pressure calibrator

f_{reg} - Uncertainty from regression. May be assumed to be in the order of $\pm 0.05\%$ according to the ISO 7066

f_{p_d} - Relative random uncertainty for the mean value of the sample for each point of calibration. This can be found in the calibration certificate for the sensor (see below).

$f_{\Delta p_{in}}$ - Uncertainty due to uncertainties in the height difference between the sensor center and the actual place of the measurements. Assumed to be insignificant compared to the other three.

The relative systematic uncertainty may now be found by taking the root mean square of all of the above uncertainties:

$$f_{cal} = \sqrt{f_{ab}^2 + f_{reg}^2 + f_{p_d}^2 + (f_{\Delta p_{in}}^2)} \tag{G.1.1}$$

In addition to the systematic uncertainty the random uncertainty of a sample has to be taken into account. This may be found by computing the mean value and the standard deviation of a sample. The standard deviation of the sample may be found using the expression below:

$$S_Y = \sqrt{\frac{\sum_{i=1}^{n}(Y_i - \bar{Y})^2}{n-1}} \tag{G.1.2}$$

Here n is the number of samples per data point. The confidence interval of the measurements is now given by the Student-t distribution:

$$\bar{Y} \pm t \cdot S_Y \tag{G.1.3}$$

The Student-t t may now be found in an look-up table based on the amount of measurements for each point. The confidence interval of the mean will now be found in the area of:

The upper and lower bounds of the measured point will now be:

$$\bar{Y} - \frac{t \cdot S_Y}{\sqrt{n}} \quad < \quad Y \quad < \quad \bar{Y} + \frac{t \cdot S_Y}{\sqrt{n}} \tag{G.1.4}$$

The uncertainty of this sample may now be gives as:

$$f_Y = t \frac{S_Y}{\sqrt{n} \cdot \bar{Y}} \tag{G.1.5}$$

The total uncertainty of the sample may now be computed as:

$$f_{tot} = \sqrt{f_Y^2 + f_{cal}^2} \tag{G.1.6}$$

Table G.1: t-value for a reduced number of sample based on a 95% confidence interval [21]

Number of samples	t
1	12.706
10	2.228
20	2.086
30	2.042
40	2.021
60	2.000
120	1.980
∞	1.960

CALIBRATION REPORT

CALIBRATION PROPERTIES
Calibrated by: Bjarne Vaage
Type/Producer: Druck
SN: V01233/12
Range: 0-100
Unit: bar a

CALIBRATION SOURCE PROPERTIES
Type/Producer: Pressurements deadweight tester P3223-1
SN: 66256
Uncertainty [%]: 0,01

POLY FIT EQUATION:
$Y = -2{,}49596994E{+}3 X^0 + 1{,}25152426E{+}3 X^1$

CALIBRATION SUMARY:
Max Uncertainty   : 0,013380 [%]
Max Uncertainty   : 0,304149 [bar a]
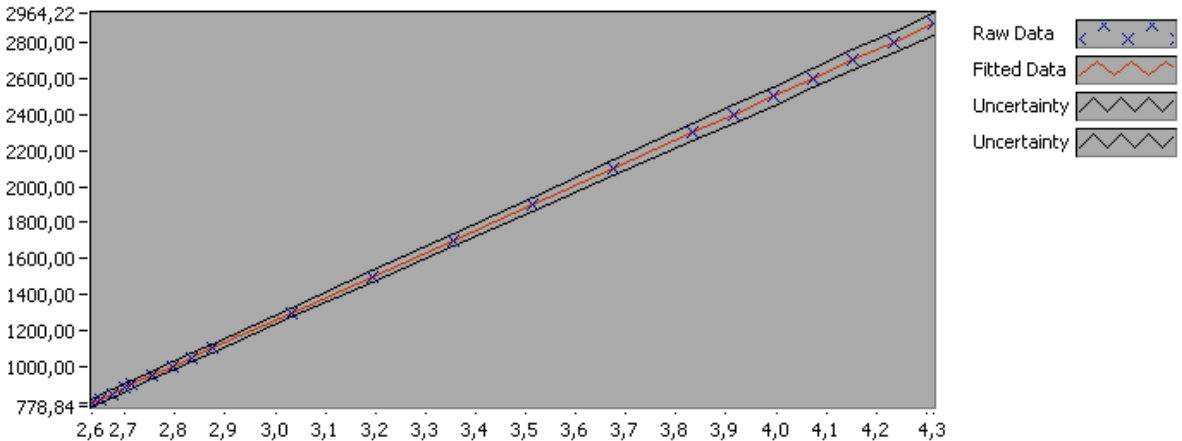RSQ   : 1,000000
Calibration points : 21

Figure 1 : Calibration chart (The uncertainty band is multiplied by 200)

Bjarne Vaage

CALIBRATION VALUES

Value [bar a]	Voltage [V]	Best Poly Fit [bar a]	Deviation [bar a]	Uncertainty [%]	Uncertainty [bar a]
800,377497	2,633772	800,259380	0,118116	0,013380	0,107088
820,407711	2,649924	820,474845	-0,067134	0,013159	0,107961
850,453032	2,673767	850,314650	0,138382	0,012865	0,109410
880,498353	2,697881	880,493450	0,004903	0,012602	0,110960
900,528568	2,713859	900,490579	0,037989	0,012445	0,112071
950,604103	2,753801	950,479117	0,124986	0,012092	0,114946
1000,679639	2,793819	1000,561762	0,117877	0,011795	0,118033
1050,755174	2,833936	1050,769411	-0,014237	0,011551	0,121378
1100,830710	2,874069	1100,996921	-0,166212	0,011341	0,124844
1301,132851	3,034013	1301,171142	-0,038290	0,010795	0,140458
1501,434993	3,194183	1501,627044	-0,192051	0,010517	0,157910
1701,737135	3,354197	1701,888398	-0,151263	0,010391	0,176831
1902,039277	3,514176	1902,106639	-0,067362	0,010349	0,196835
2102,341419	3,674188	2102,365696	-0,024276	0,010349	0,217565
2302,643561	3,834217	2302,645026	-0,001465	0,010365	0,238658
2402,794632	3,914211	2402,760245	0,034387	0,010380	0,249402
2502,945703	3,994320	2503,018922	-0,073219	0,010401	0,260343
2603,096774	4,074370	2603,202763	-0,105989	0,010416	0,271147
2703,247845	4,154256	2703,182811	0,065034	0,010438	0,282168
2803,398916	4,234253	2803,300558	0,098358	0,010460	0,293238
2903,549987	4,314226	2903,388521	0,161465	0,010475	0,304149

COMMENTS:

The uncertainty is calculated with 95% confidence. The uncertainty includes the randomness in the calibrated instrument during the calibration, systematic uncertainty in the instrument or property which the instrument under calibration is compared with (dead weight manometer, calibrated weights etc.), and due to regression analysis to fit the calibration points to a linear calibration equation.The calculated uncertainty can be used as the total systematic uncertianty of the calibrated instrument with the given calibration equation.

H | Reverse engieneering of the runner dimensions in Bruvollelva

In order to model the behavior of Bruvollelva power plant the dimensions of the runner is needed. The data sheet from the producer is rather sparse with on information so most of the main dimension has to be calculated in terms of modeling the behavior. The dimensions giver in the data sheet are:

Property	Value	[unit]	Comment
D_2	0.9	$[m]$	
Q_R	3.465	$[m^3/s]$	0.9 Q_{max}
H_R	110	$[mWc]$	
n	750	[rpm]	

By using the method described in *Pumper & Turbiner* by Hermod Brekke the rest of the dimensions of the turbine can be reversed engineered and used for the simulation. For this to work a couple of assumptions has to be made. The reduced inlet peripheral velocity of the runner usually is in the magnitude of 0.70 - 0.75 where that larges value corresponds to the most high head runners. With a design head of 110 mWc a $\underline{u}_1$ of 0.71 seems appropriate. Again, by assuming a rated hydraulic efficiency, η_{h_R}, of 0.96 the whole velocity triangle at the inlet may be calculated. The velocity components at the inlet now becomes:

$$u_1 = \underline{u}_1 \cdot \sqrt{2g H_R} = 32.98 \, m/s$$

$$c_{u_1} = \frac{\eta_{h_R}}{2\underline{u}_1} = 32.41 \, m/s$$

The last velocity component, c_{m_1}, still needs to be calculated. A quite normal assumption here is to assume this equal to the c_m -component at the outlet. The components may now be calculated as:

$$c_{m_1} = c_{m_2} = \frac{Q_R}{\pi D_2^2/4} = 5.45 \, m/s$$

With the velocity components in check the dimension at the inlet may be calculated. The inlet diameter, D_1, can be calculated by the rotational speed and the u_1-component. And with the inlet

diameter known the inlet height of the runner can be calculated by using the continuity equation:

$$D_1 = \frac{u_1 \cdot 60}{\pi \, n} = 0.84 \, m$$

$$B_1 = \frac{D_2^2}{4 \, D_1} = 0.24 \, m$$

Now all that is left is to calculate the guide vane angle at the inlet as well as the blade angles at both inlet and outlet. These are needed for calculating the starting torque of the runner and is for that matter quite important for the simulation. These may be calculated as:

$$\alpha_1 = \tan^{-1}\left(\frac{c_{m_1}}{c_{u_1}}\right) = 9.8°$$

$$\beta_1 = \tan^{-1}\left(\frac{c_{m_1}}{u_1 - c_{u_1}}\right) = 73.9°$$

$$\beta_2 = \tan^{-1}\left(\frac{c_{m_2}}{u_2}\right) = 8.8°$$

I | Risk assesment

NTNU			Risikovurdering		Utarbeidet av	Nummer	Dato
HMS /KS					HMS-avd.	HMSRV2603	04.02.2011
					Godkjent av	Side	Erstatter
					Rektor		09.02.2010

Enhet: _____   **Dato:** _____

Linjeleder: Olav Bolland   IVT / EPT   07.04.2016

Deltakere ved risikovurderingen (m/ funksjon):
(Ansv. veileder, student, evt. medveiledere, evt. andre m. kompetanse)

Bjarne Vaage (student på feltforsøk)

Risikovurderingen gjelder hovedaktivitet: Masteroppgave student Bjarne Vaage, Simulation of hydraulic transients of operation at two hydro power plants

Signaturer: Ansvarlig veileder: _____   Student: _____

ID nr.	Aktivitet/prosess fra kartleggingsskjemaet	Mulig uønsket hendelse	Vurdering av sann- synlighet (1-5)	Vurdering av konsekvens				Risiko- verdi (menn- eske)	Kommentarer/ status Forslag til tiltak
				Menneske (A-E)	Ytre miljø (A-E)	Øk/ materiell (A-E)	Om- dømme (A-E)		
1	Reise til og fra Snåsa	Kollisjon/utforkjøring	2	D	B	B	B	D2	Norsk lov etterleves
2	Opphold i Bruvollelva kraftverk	Støy, vannsprut, fall	1	C	A	B	B	C1	Personlig verneutstyr bæres alltid
3	Feltmålinger i Bruvollelva kraftverk	Vannsprut, fall	1	C	A	C	B	C1	Personlig verneutstyr bæres alltid
4	Oppkobling av DIP-lab	Klemfare, berøring av spenningssatt punkt	1	D	A	A	C	D1	Personlig verneutstyr bæres alltid, holde god avstand ved krandrift, holde avstand når spenning er påsatt
5									
6									